From THE INSTITUTE OF ENVIRONMENTAL MEDICINE
Karolinska Institutet, Stockholm, Sweden

PHYSIOLOGICALLY BASED MODELLING OF NANOPARTICLE BIODISTRIBUTION AND BIOKINETICS

Ulrika Carlander

Stockholm 2016

Published by Karolinska Institutet.
Printed by AJ E-Print AB

ISBN 978-91-7676-487-9

Physiologically Based Modelling of Nanoparticle Biodistribution and Biokinetics

THESIS FOR DOCTORAL DEGREE (Ph.D.)

By

Ulrika Carlander

Principal Supervisor:
Professor Gunnar Johanson
Karolinska Institutet
Department of Environmental Medicine
Division of Work Environment Toxicology

Co-supervisor(s):
Associate Professor Hanna Karlsson
Karolinska Institutet
Department of Environmental Medicine
Division of Biochemical Toxicology

Professor Lennart Lindbom
Karolinska Institutet
Department of Physiology and Pharmacology
Division of Microvascular Physiology

Opponent:
Professor Michèle Bouchard
Université de Montréal
Department of Environmental and Occupational Health
School of Public Health

Examination Board:
Professor Mats Karlsson
Uppsala University
Department of Pharmaceutical Biosciences
Division of Pharmacometrics

Associate Professor Tommy Cedervall
Lund University
Department of Biochemistry and Structural Biology

Associate Professor Louiza Bohn Thomsen
Aalborg University
Department of Health Science and Technology

ABSTRACT

To predict the toxicity of nanoparticles (1-100 nm), it is crucial to understand their biokinetics i.e. how they are taken up, distributed, dissolved and removed from the body. Such information can be gained from biodistribution studies in animals. However, to make predictions for other types of nanoparticles, exposure conditions and species, including humans, extrapolations from such studies are required. Use of models, such as physiologically based pharmacokinetic (PBPK) models, makes extrapolations feasible, given that the models are sufficiently validated.

In this thesis, a conceptual nanospecific PBPK model for intravenous administration to rats was developed and applied to different types of inert nanoparticles using experimental data from recent scientific publications (Papers I and II). The model represents systemic distribution and serves as a foundation for expansion to other species and other exposure routes (inhalation, dermal, oral). The PBPK simulations suggest that the model is able to describe the biokinetics of different types of inert nanoparticles given intravenously despite large differences in properties and exposure conditions. Our model is the first to include separate compartments for phagocytic cells and saturable phagocytosis. The simulations show that (1) phagocytosis needs to be incorporated in nano PBPK models, (2) the dose has a clear impact on biokinetics, but (3) further refinements are needed to better reflect processes such as agglomeration, corona formation and dissolution. The model was slightly modified to describe the biodistribution and biokinetics of nanoceria of different sizes and administered via other routes (Paper III). While the model could well predict the biokinetics after intravenous dosing, the predictions of inhalation, instillation and ingestion data were poor. The poor agreement may be partly due to low absorption via these routes, resulting in low nanoceria levels in tissues and organs, often close to or below the detection limit, in tissues. However, low absorption is hardly the only explanation, as the experimentally observed concentration time courses of nanoceria in tissues suggest that the biokinetics depend not only on the nanoparticle properties (size, coating) but also on the exposure conditions (dose, exposure route). The PBPK model was further developed to account for the complexity of inhalation exposure to nanoparticles (Paper IV). The modified model includes regional particle deposition in the respiratory tract, mucociliary clearance and phagocytosis in the lungs, olfactory uptake, and transport into the systemic circulation by alveolar wall translocation. The PBPK model described the biodistribution well and again suggested phagocytosis to be very important.

The PBPK simulations were performed assuming that the nanoparticles are inert, *i.e.* do not dissolve or degrade in the body. However, when modelling the experimental data it seemed that the biokinetics might be better explained by introducing dissolution in the PBPK model. A related problem is that most experimental studies of metal nanoparticles use elemental analysis such as inductively coupled plasma mass spectrometry (ICP-MS). Such analyses do not discriminate between different forms of metal and therefore obscures the biokinetics. To test if gold nanoparticles dissolve in biological media, we developed an in vitro method to characterize dissolution of gold nanoparticles in contact with cell medium, macrophages and lipopolysaccharide (LPS)-triggered macrophages, simulating a disease state (Paper V). We demonstrated that gold nanoparticles are dissolved by cell medium and macrophages and even more so by LPS-triggered macrophages. The dissolution rate was higher for 5 nm than for 50 nm gold particles.

SVENSK SAMMANFATTNING

För att kunna förstå och förutse om nanopartiklar (1-100 nm) kan skada människor, är det viktigt att ha kunskap om nanopartiklars biokinetik d.v.s. hur de tas upp, distribueras, bryts ner i och utsöndras ur kroppen. Denna typ av information kan vi få från biodistributionsstudier på djur. För att göra prognoser för andra typer av nanopartiklar, exponeringsförhållanden och arter, inklusive människor, behöver vi oftast göra extrapoleringar utifrån den information vi har. Användning av tillräckligt validerade modeller, såsom fysiologiskt baserade farmakokinetiska (PBPK) modeller möjliggör sådana extrapoleringar.

I denna avhandling har en konceptuell PBPK modell för intravenöst administrerade nanopartiklar i råttor utvecklats och tillämpats på olika typer av stabila partiklar med hjälp av experimentella data hämtade från vetenskapliga publikationer (Studie I och II). Modellen representerar systemisk distribution och fungerar som bas för expansion till andra arter och andra exponeringsvägar (inandning, oralt, via huden). PBPK simuleringar visar att modellen kan beskriva biokinetiken för olika typer av stabila nanopartiklar som administreras intravenöst, trots stora skillnader i egenskaper och exponeringsförhållanden. Vår modell är den första att inkludera modellstrukturer för fagocyterande celler och deras upptagsprocesser. Simuleringarna visar att (1) fagocytos borde inkluderas i PBPK modeller för nanopartiklar, (2) dosen har en tydlig påverkan på biokinetik, men (3) ytterligare förbättringar behövs för att bättre återspegla processer såsom agglomerering, koronabildning och nedbrytning. Modellen ändrades något för att kunna beskriva biodistribution och biokinetik av nanoceria med olika storlekar och administrerade via olika exponeringsvägar (Studie III). Medan modellen väl förutsåg biokinetik för intravenös dosering så beskrev modellen kinetiken dåligt för inandning, instillation och förtäring. Den dåliga modellanpassningen kan delvis bero på låg absorption via dessa exponeringsvägar, vilket leder till låga nivåer av nanoceria i organ, ofta nära eller under detektionsgränsen. Låg absorption är troligen inte den enda förklaringen, eftersom tidsförloppen i experimentella data tyder på att biokinetik utöver nanopartiklars egenskaper (storlek, beläggning) också påverkas av exponeringsförhållandena (dos, exponeringsväg). PBPK modellen vidareutvecklades för att bättre beskriva den komplexa inhalationsexponeringen. Modellen inkluderar regional deponering av partiklar i luftvägarna, mukociliär transport och upptag i alveolära makrofager, transport via luktnerv till hjärna och upptag från lunga till blod (Studie IV). Modellen beskrev biokinetiken för nanoceria väl och visade igen på vikten av fagocytos som en del i PBPK modeller för nanopartiklar.

Våra PBPK simuleringar utfördes med antagande om att partiklarna var stabila, d.v.s. de bröts inte ner i kroppen. När vi utförde modellsimulering på experimentella data för bl.a. nanopartiklar av guld så verkade det som om biokinetiken troligen bättre skulle kunna förklaras om nedbrtyning inkluderades i modellen. Ett relaterat problem är att de flesta experimentella biodistributionsstudier med nanopartiklar i metall använder elementaranalys, såsom induktivt kopplad plasma-masspektrometri (ICP-MS), för att analysera mängd metall i organ. Denna typ av analys kan inte särskilja olika former av metall och därmed inte heller skillnader i biokinetik mellan dessa. För att testa om nanopartiklar av guld bryts ner i biologisk miljö, utvecklade vi en *in vitro*-metod för att undersöka om nanopartiklar i guld bryts ner i kontakt med cellmedium, makrofager och lipopolysackarid (LPS) -stressade makrofager (Studie V). Vi visade att guldpartiklarna bryts ner av cellmedium och av makrofager, och ännu mer om makrofagerna stressades med LPS. Nedbrytningen var snabbare för 5 nm än för 50 nm stora guldpartiklar.

LIST OF SCIENTIFIC PAPERS

This thesis is based on the following publications:

I. Dingsheng Li, Gunnar Johanson, Claude Emond, **Ulrika Carlander**, Martin Philbert, Olivier Jolliet
Physiologically based pharmacokinetic modeling of polyethylene glycol-coated polyacrylamide nanoparticles in rats.
Nanotoxicology, 2014, 8(S1), 128-137.

II. **Ulrika Carlander**, Dingsheng Li, Claude Edmond, Jolliet Olivier, Gunnar Johanson
Toward a general physiologically-based pharmacokinetic model for intravenously injected nanoparticles.
International Journal of Nanomedicine, 2016, 11, 625-640.

III. **Ulrika Carlander**, Tshepo Paulsen Moto, Anteneh Assefa Desalegn, Robert Yokel and Gunnar Johanson
Modelling biokinetics of nanoceria injected intravenously into rats.
Manuscript.

IV. Dingsheng Li, Masako Morishita, James G Wagner, Mohammad Fatouraie, Margaret Wooldridge, W. Ethan Eagle, James Barres, **Ulrika Carlander**, Claude Emond, Olivier Jolliet
In vivo biodistribution and physiologically based pharmacokinetic modeling of inhaled fresh and aged cerium oxide nanoparticles in rats.
Particle and Fibre Toxicology, 2016, (epub ahead, DOI: 10.1186/s12989-016-0156-2).

V. **Ulrika Carlander**, Klara Midander, Yolanda Hedberg, Matteo Bottai, Gunnar Johanson, Hanna Karlsson
Triggered macrophages can dissolve gold nanoparticles.
Manuscript

The publications are referred to by roman numerals (I-V) in the thesis text. The articles are reproduced in full text as appendices.

CONTENTS

LIST OF ABBREVIATIONS

Ad	Adrenal gland
AIC	Akaike information criterion
AM	Alveolar macrophages
BIC	Bayesian information criterion
Bl	Blood
BM	Bone marrow
Bo	Bone
Br	Brain
C^{14}	Carbon-14 radioactivity
CeO_2	Cerium dioxide
Co_3O_4	Cobalt oxide
CTAB	Cetyltrimethylammonium bromide
D	Diameter
DLS	Dynamic light scattering
DNA	Deoxyribonucleic acid
F	Faeces
Fa	Fat
GIT	Gastrointestinal tract
He	Heart
ICP	Inductively coupled plasma
Ki	Kidney
L	Length
Li	Liver
LPS	Lipopolysaccharides
Lu	Lung
Lymp	Lymph nodes
MAPE	Mean absolute percentage error
MINP	Magnetic imaging nanoparticles
MS	Mass spectrometry
Mu	Muscle
NP	Nanoparticle
PAA	Polyacrylamide
PBPK	Physiologically based pharmacokinetics

PC	Phagocytic cells
PEG	Polyethylene glycol
PLGA	Poly(lactic-co-glycolic acid)
PS	Polystyrene
PT-ODN	Phosphorothioate oligonucleotide
QD	Quantum dots
R^2	Coefficient of determination
ROS	Reactive oxygen species
SF	Spinal fluid
SFMS	Sector field mass spectrometry
Sk	Skin
Sp	Spleen
Tb_2O_3	Terbium oxide
Te	Testis
TEM	Transmission electron microscopy
TiO_2	Titanium dioxide
Ty	Thymus
U	Urine

1 INTRODUCTION

Nanotechnology is an innovative and evolving field where new products are continuously introduced on the market. In the healthcare and medicine sector alone, the global market is estimated to increase from $30 billion in 2014 to $80 billion in 2019 (James *et al.*, 2014). The benefits with nanotechnology are numerous and provide hope for solving many global problems such as diseases, global warming, and shortage of water and food.

Particles of a nanometre scale, often called nanoparticles, have unique properties, including superparamagnetism, catalytic activity and durability, as well as unexpected optical characteristics and increasing the strength of materials. For these reasons, nanoparticles have become popular components of products and contribute to the improvement in many sectors, such as information technology, energy, transportation, construction, environmental science, medicine, and food (Lee *et al.*, 2010; Duncan, 2011; Parveen *et al.*, 2012; Raj *et al.*, 2012; Wang *et al.*, 2012; Waser, 2012; Qu *et al.*, 2013).

To ensure a continuous and sustainable development, nanoparticles must be safe for humans and the environment. Meanwhile, the increasing use of nanoparticles increases the likelihood of exposure and thereby the risk for unintended consequences to human health and the environment. In addition to intentional exposure, *e.g.* when used in pharamceutical applications, and unintentional expsoure during manufacturing, use and disposal, nanoparticles may be released from products, resulting in secondary human exposure via the skin, lungs, eyes and or mouth (Buzea *et al.*, 2007; Nowack *et al.*, 2013; Liou *et al.*, 2015). Great efforts have been made to evaluate the health effects of nanomaterials on humans, but the results are inconclusive so far (Sharifi *et al.*, 2012; Liou *et al.*, 2015; Zhang *et al.*, 2015). Most studies have been carried out *in vitro* and with animals. Data from exposed humans are rare although the number of epidemiological studies is increasing (Liou *et al.*, 2015).

Because of their extremely small size, similar to that of the structural elements of cells, there is concern that nanoparticles may be toxic, as has indeed been reported in both *in vitro* and *in vivo* studies (Buzea *et al.*, 2007; Krug *et al.*, 2011; Kermanizadeh *et al.*, 2015). To exert toxicity, these particles must reach the cell, *i.e.*, become bioavailable in sufficiently high amounts. Several methods provide valuable information concerning the absorption, distribution, metabolism (degradation/dissolution) and excretion of nanoparticles. *In vitro* studies give insight into the mechanisms of action of various cellular processes; whereas *in vivo* studies can be employed to characterize the biodistribution in living animals (Marquis *et al.*, 2009). Furthermore, *in silico* tools such as physiologically based pharmacokinetic (PBPK) models can be used to combine *in vitro* and *in vivo* data with an aim of predicting the final outcome in terms of the relation between exposure/dose and health effects (Krishnan *et al.*, 2010; Johanson, 2014).

The advantage of PBPK modelling is that toxicological data can be extrapolated from animals to humans, from high to low doses and between different routes of exposure, without additional *in vitro* and/or *in vivo* investigations (IPCS, 2010; Krishnan *et al.*, 2010; Johanson, 2014). However, only a few PBPK models have been published for nanoparticles to date and these are difficult to apply to other types of nanoparticles and exposure conditions because their physiological basis is limited (Li *et al.*, 2010; Bachler *et al.*, 2013; Kolanjiyil *et al.*, 2013; Lin *et al.*, 2015b; Johanson *et al.*, 2016). More physiologically relevant models are required for trustworth extrapolations.

2 BACKGROUND

2.1 NANOPARTICLES

Nanoparticles are small, with sizes similar to the structural elements of cells, antibodies, proteins and viruses. A common definition is any shape with dimensions between 1 to 100 nm, but this may vary depending on regulatory framework (ISO, 2008; European Commission, 2011; FDA, 2014). They occur naturally, but are also produced by humans, on purpose or inadvertently (Buzea *et al.*, 2007).

Nanoparticles can be distributed in gaseous form, as liquids or deposited on solid materials and their properties can be tailored to have extraordinary characteristics, different from molecules and bulk materials (Roduner, 2006). One such characteristic is enhanced quantum and plasmon effects, giving nanoparticles intense colours useful for biological imaging and sensing (Michalet *et al.*, 2005; Scholl *et al.*, 2012). Another property is superparamagnetism, which makes nanoparticles susceptible to magnetic fields and hence valuable for MRI imaging, data storage and wastewater treatment *etc.*(Frey *et al.*, 2009; Reddy *et al.*, 2012; Xu *et al.*, 2012; Qu *et al.*, 2013). A third property is chemical activity, and this, together with increased surface area to volume ratio, makes nanoparticles excellent catalysts (Guo *et al.*, 2013; Liu *et al.*, 2014). Typically, properties are tuned by changing particle size, geometry, and chemistry. Therefore, information about the nanoparticles' physicochemical properties is crucial in nanoparticle design, applications, and risk assessment.

However, physicochemical characterization of nanoparticles is challenging and may change with environment and exposure conditions (Oberdorster *et al.*, 2005a; Fadeel *et al.*, 2015). To open for proper interpretation of results from toxicity and biodistribution studies, the Organization for Economic Co-operation and Development (OECD) recommends that nanoparticles are characterized at least as received from the suppliers, administrated and *in situ* (OECD, 2012). However, this is rarely carried out in research studies. Properties of importance to characterize are: size, size distribution, surface area, shape, crystal structure, chemical composition, surface charge, surface energy, surface coatings, solubility, agglomeration state and impurities. All these parameters have been reported to modify toxicity and biodistribution (Oberdorster *et al.*, 2005a; Aillon *et al.*, 2009; Nel *et al.*, 2009; Hussain *et al.*, 2015). In this thesis, the focus is on engineered nanoparticles that are considered inert.

2.1.1 Toxicity

The toxicity of nanoparticles depends on their physicochemical characteristics and how they interact with cellular and molecular substances in the body (Aillon *et al.*, 2009; Nel *et al.*, 2009; Zhu *et al.*, 2010). Nanoparticles can absorb and release substances, and can join together to form agglomerates (loosely attached group of particles) or aggregates (tightly attached group of particles) (Jiang *et al.*, 2009; Gliga *et al.*, 2014). Moreover, they can catalyse or participate in chemical and biological reactions (Daniel *et al.*, 2004). As a result of this dynamic interaction, the particle identity and its hazard potential may change with time and environment.

Through their surfaces, nanoparticles interact with the surrounding environment and their surfaces are potentially more reactive compared with larger particles because of increased surface area to volume ratio. Actually, surface area has been proposed to be a better dose

metric for toxicity than mass or number of nanoparticles (Oberdorster *et al.*, 2005b; Braakhuis *et al.*, 2016; Schmid *et al.*, 2016). Despite this, mass is probably the most commonly used dose metric in toxicity studies and volume has been used to describe the overload phenomenon caused by inhaled nanoparticles (Morrow, 1988; Pauluhn, 2014; Kermanizadeh *et al.*, 2015).

As a consequence of the wide range of nanoparticle properties, toxicity and mechanisms of toxicity differ considerably. *In vitro* studies show that nanoparticles can trigger a variety of toxicological mechanisms, such as release of reactive oxygen species (ROS), DNA damage, inflammatory effects and cell death through various mechanisms including autophagy (Stern *et al.*, 2012; Gliga *et al.*, 2014; Magdolenova *et al.*, 2014). Sometimes the toxicity is not related to the nanoparticles themselves, but rather to the release of other substances, as observed for some metallic nanoparticles through a process called "The Trojan horse effect", *i.e.* when cells take up nanoparticles, which release metallic ions inside the cells and cause toxicity (Limbach *et al.*, 2007). Another effect is the presence in nanoparticles of endotoxins that can induce inflammation (Vallhov *et al.*, 2006). Excessively high concentrations are often used *in vitro* and hence do not always reflect environmental exposures accurately (Krug *et al.*, 2011).

In vivo, toxicity has been investigated after exposure to nanoparticles via inhalation, instillation, and dermal, oral, intraperitoneal and intravenous routes (Kermanizadeh *et al.*, 2015). The majority of the studies focus on animals and short-term exposure. Only a few studies included repeated and long-term exposure and long post-exposure follow-up times. The number of epidemiological studies is small, but growing (Liou *et al.*, 2015). Studies indicate health effects related to exposure to nanomaterials, such as increased expression of cardiovascular and oxidative biomarkers, reduced levels of antioxidant enzymes, allergic dermatitis and increased sneezing as an indicator of airway irritation. However, most of these studies are cross-sectional and cover small numbers of participants, low exposures and short intervals between exposure and effect. In addition, exposure assessments are inconsistent and only a few types of nanoparticles have been covered. On the other hand, nanotoxicology is linked to particle and fibre toxicology and lessons learned from this field on ultrafine particles are relevant for nanoparticles as well, such as deposition pattern, particle overload in the lung, and particle toxicity as oxidative stress, cardiovascular diseases and the fibre paradigm (Oberdorster *et al.*, 2005b; Donaldson *et al.*, 2012; Grosse *et al.*, 2014; Borm *et al.*, 2015).

Despite low uptake in the body via inhalation, skin contact and ingestion, adverse effects in a variety of distal organs have been reported (Kermanizadeh *et al.*, 2015). Locally the deposition of nanoparticles may be higher and contributes to the toxicity (Balashazy *et al.*, 2003). In human and animal inhalation studies, nanoparticles have induced inflammation, pulmonary fibrosis, granuloma formation, cardiovascular effects and lung tumours (Brook, 2008; Kermanizadeh *et al.*, 2015). Oral studies in rats with nanoceria demonstrate effects on distal organs such as liver, brain and kidney (Kumari *et al.*, 2014a; Kermanizadeh *et al.*, 2015). Results from repeated dermal exposure in guinea pigs of silver nanoparticles suggest cardiotoxicity, nephrotoxicity and osteotoxicity (Korani *et al.*, 2011; Kermanizadeh *et al.*, 2015). Much like in studies *in vitro*, the doses used are often far higher than expected human exposure. Dissolved and released entities can also contribute to the observed toxicity (Park *et al.*, 2010; Gliga *et al.*, 2014). In short and as expected, toxicity differs widely depending on nanoparticle properties and exposure conditions. Several on-going efforts are made to group nanomaterials for testing, read-across, risk assessments and safety-by-design (Arts *et al.*, 2015; Geraci *et al.*, 2015; EU NanoSafety Cluster, 2016; OECD, 2016).

Oxidative stress is commonly induced by nanoparticles through many different mechanisms as a result of the particles' intrinsic properties or by interaction with cells (Nel *et al.*, 2006; Xia *et al.*, 2006; Manke *et al.*, 2013). Surface reactivity is an intrinsic property and may be involved in the production of reactive oxygen species via oxidation and Fenton-like processes. When nanoparticles interact with cells like macrophages and neutrophils, the cells may respond by release of oxygen species in an attempt to remove the particles and/or signal stress. Reactive oxygen species are, on the other hand, produced endogenously during vital processes like cell breathing and oxidative burst, in which superoxide ($O2^-$, $HO2^\bullet$), hydrogen peroxide (H_2O_2) and hydroxyl radicals ($^\bullet OH$) are formed (Halliwell *et al.*, 2015). To neutralize the reactive oxygen species and protect itself from injuries, the cell uses antioxidant enzymes and proteins, such as glutathione, vitamins C and D, superoxide dismutase, and peroxidase. If the production of reactive oxygen species gets too high the redox homeostasis is disturbed, which may result in membrane lipid peroxidation, stress signalling, cell pathogenesis, and, ultimately, cell death. Uncontrolled oxidative stress can result in inflammation and progress into cardiovascular diseases, pulmonary fibrosis and tumour formation.

2.1.2 *In vivo* biodistribution

The target dose determines the toxicity. Correlating exposure to target dose information about biokinetics is essential. Biokinetics describes how nanoparticles are taken up, transported, dissolved and removed from the body over time and are based on biodistribution studies. In biodistribution studies mass-time deposition in tissues and organs is measured and target organs are identified. Consumer, patient and worker exposure can occur via inhalation and oral, dermal and intravenous routes, for instance.

2.1.2.1 Intravenous exposure

Intravenous exposure represents 100 % bioavailability and serves as a reference for the biokinetics of nanoparticles via other mechanisms, such as inhalation, dermal or oral routes. In addition, it is the most likely potential route of exposure for nanoparticles as therapeutic agents, as absorption is often negligible via other routes.

When nanoparticles are administrated intravenously, the majority of them are usually distributed to organs belonging to the mononuclear phagocyte system (MPS), especially the liver and spleen (Saba *et al.*, 1969). In the mononuclear phagocyte, system nanoparticles are captured by phagocytic cells like macrophages and Kupffer cells. Nanoparticles are also distributed to other organs, but to a lesser extent. In addition, uptake by cell types other than phagocytic cells has been observed, as well as attachment to cell surfaces and deposition in the extracellular space (Demoy *et al.*, 1999; van Schooneveld *et al.*, 2008; Hirn *et al.*, 2011; Keene *et al.*, 2012).

As soon as the nanoparticles are in contact with blood, proteins and other biomolecules instantly begin competing over binding to the nanoparticle in a process called opsonisation, leading to the formation of a protein corona (Nel *et al.*, 2009; Docter *et al.*, 2015). The protein corona changes the biological property of the nanoparticles and modifies the recognition and phagocytosis by macrophages (Docter *et al.*, 2015). Hydrophobic and charged particles appear to be opsonised more easily than uncharged hydrophilic nanoparticles such as PEG coatings. Coating with PEG tends to minimize opsonisation and

uptake by the MPS (Bazile *et al.*, 1995; Schottler *et al.*, 2016). In fact, opsonisation affects distribution and uptake mechanisms (Ogawara *et al.*, 2001; Tenzer *et al.*, 2013).

To reach the tissue, nanoparticles have to be distributed by the blood circulation to the organs and locally cross the endothelium (Figure 1). To cross the endothelium the nanoparticles have to pass between the endothelial cells or through them (Setyawati *et al.*, 2015). To keep the barrier function, endothelial cells are linked to each other with junctions (Michel *et al.*, 1999; Mehta *et al.*, 2006). The junctions are tight in the brain, but in organs like the liver and bone marrow there are fenestrations, which facilitate translocation into tissue. Some nanoparticles have the ability to interact with junctions, which increases the transport to tissue (Moyes *et al.*, 2007; Lin *et al.*, 2012). During inflammation, tight junctions are loosened and endothelium gaps are formed in the normally continuous endothelium coated with glycocalyx *i.e.* a hairy coating made of glycoprotein-polysaccharide that covers the luminal side of the endothelium (Levick, 2010).

Transcellular passage of nanoparticles can occur by different mechanisms, such as endocytosis and diffusion, see Figure 1. Endocytosis requires energy and includes processes like phagocytosis, caveolae-mediated or clathrin-mediated endocytosis and macropinocytosis with diversified characteristics (Nel *et al.*, 2009; Canton *et al.*, 2012). The uptake to cells involves several steps, such as transport toward the surface, recognition by cells, binding and cell internalization (Jin *et al.*, 2009; Ohta *et al.*, 2012; Feliu *et al.*, 2016b). The capacity for endocytosis in capillaries is higher in organs like liver and bone marrow (Sarin, 2010). These organs are called sinusoid reticuloendothelial blood capillaries (Saba, 1970). Recently a new pathway for translocation of nanoparticles over the endothelium has been observed, called membrane nanotubes, which are formed between cells with diameters ranging between 50-200 nm in average (Rehberg *et al.*, 2016).

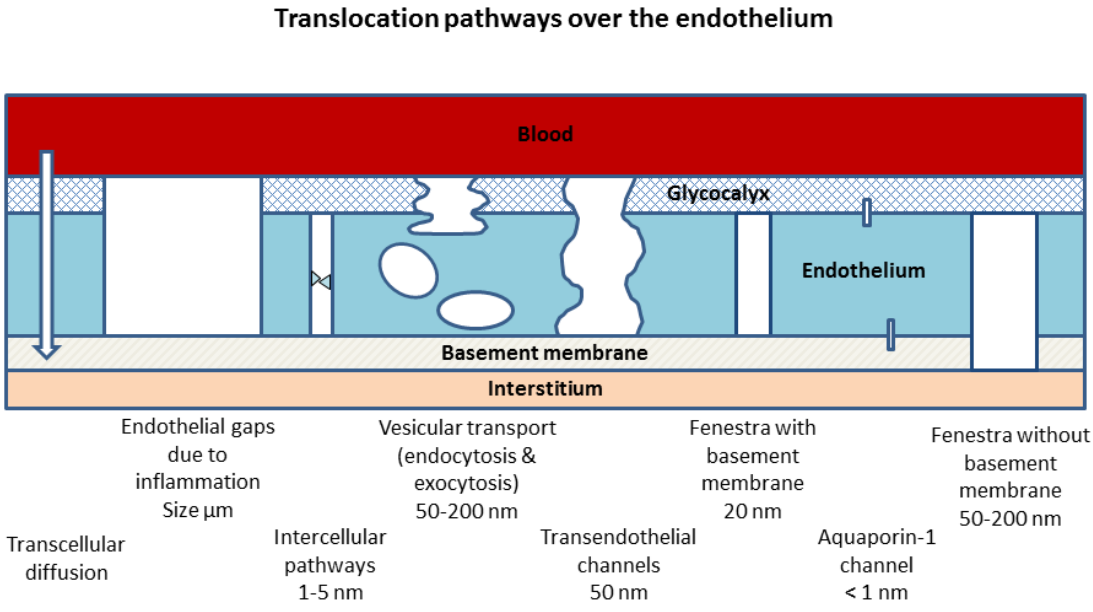

Figure 1. Translocation pathways over the endothelium.

It has long been known that the uptake capacity of the liver can be suppressed by saturating the Kupffer cells or by depleting opsonic factors (Biozzi *et al.*, 1953; Bradfield, 1980; Illum *et al.*, 1986). When phagocytosis in the liver is suppressed, accumulation of particles increases in spleen, lung, kidney and bone marrow (Biozzi *et al.*, 1953; Illum *et al.*, 1987).

The saturation may be due to either the equilibrium between endocytosis and exocytosis or the capacity limitation of the cells.

The fate within the cell varies depending on the uptake process. In the studies where internalization of nanoparticles was evaluated, most nanoparticles were found in vesicles, lysosomes and endosomes (Moghimi, 2002; Lee *et al.*, 2009a; Wang *et al.*, 2010; Morais *et al.*, 2012). In the lysosomes and phagosomes, nanoparticles are subjected to an environment with enzymes, reactive oxygen species and reduced pH. Many nanoparticles are stable, but in some cases coatings and labelling may dissolve in this environment (Briley-Saebo *et al.*, 2004; Knop *et al.*, 2010; Mahon *et al.*, 2012).

The macrophages of the MPS are heterogeneous and differ slightly between species, pointing to a potential difference in the ability to recognize and capture nanoparticles (Gordon *et al.*, 2005; Verschoor *et al.*, 2012). Furthermore, the pool size and kinetic parameters, such as rate of migration, rate of production and mean turnover time of macrophages, may vary between tissues (van Furth, 1989). In addition, repeated exposure can suppress and stimulate the MPS depending on the dose, dosing frequency and dosing duration (Biozzi *et al.*, 1953).

Nanoparticles are discharged from cells by diffusion (only small nanoparticles), exocytosis or due to cell death. Observation of concentration of gold nanoparticles to fewer cells suggests that clustering and cannibalism between Kupffer cells can occur (Sadauskas *et al.*, 2009). Clearance from the body by way of urine and faeces via bile is reported. Clearance to urine has been argued to be limited to small substances (< 40 kDa) and nanoparticles (< 8 nm), but exceptions have been reported (Choi *et al.*, 2007; Lacerda *et al.*, 2008; Nel *et al.*, 2009).

2.1.2.2 Inhalation

Dust- and airborne nanoparticles can be inhaled and end up in the respiratory system. The respiratory system with its conduit airways is organized in a complex branching tree structure, which can be divided into upper respiratory tract, tracheobronchial region and alveolar region (Snipes, 1989; Oberdorster *et al.*, 2005b). When nanoparticles are inhaled they will be deposited in this system, with locally enhanced deposition in airway branches, so-called “hot spots” (Brain *et al.*, 1976; Snipes, 1989; Balashazy *et al.*, 2003).

Where nanoparticles are deposited and to what extent depends on their properties, the exposure conditions and the physiological and anatomical properties of the exposed species (Snipes *et al.*, 1983; Daigle *et al.*, 2003; Kreyling *et al.*, 2013). The three most commonly used mechanisms to describe deposition are impaction, sedimentation and diffusion (Anjilvel *et al.*, 1995; Hofmann, 2011). Because of the extremely small sizes, nanoparticle deposition is mainly driven by diffusion, by which the particles are transported deeper into the lung than larger particles. Larger particles are primarily deposited by impaction in the upper airways (> 1.5 µm) and by sedimentation in the tracheobronchial region (> 0.5 µm). Other mechanisms for deposition are turbulence, interception, electrostatic deposition, and thermophoretic and diffusiophoretic forces, but their impacts on deposition on nanoparticles are, thus far, not well-addressed in modelling (Guha, 2008).

Once deposited, nanoparticles are in contact with mucus and lining fluids where they may submerge and react with ions, surfactants and proteins. As a result, those particles may agglomerate, degrade, migrate or become engulfed by lung cells (Schulze *et al.*, 2011).

Deposited nanoparticles can be cleared. In the upper respiratory tract, they are removed by coughing, sneezing and swallowing. In the tracheobronchial region, the main mechanism is by the mucociliary escalator to the larynx and further transport into the gastrointestinal tract (Oberdörster, 1988). In the alveolar region, nanoparticles are captured by alveolar macrophages, which migrate to the tracheobronchial region for mucociliary clearance or to mediastinal lymph nodes (Geiser *et al.*, 2005; Choi *et al.*, 2010). The retention time in the alveolar region is longer than in the tracheobronchial region (Oberdörster, 1988).

Increasing the dose may overload the system and impair macrophage clearance. For poorly soluble particles impaired clearance has been suggested to start when 6 % or more of the alveolar macrophages volume in rats is occupied by particles (Morrow, 1988; Morrow *et al.*, 1996). How to extrapolate this to human exposure limit values is debated (Pauluhn, 2014; Morfeld *et al.*, 2016). During an overload situation an inflammation may result in an increased leakage of particles to the lymph nodes (Tran *et al.*, 2000). Alveolar macrophages are long-lived, but new ones can be recruited, especially during inflammation.

From the lining fluid, nanoparticles can migrate to the epithelium surface and translocate into either the blood circulation or the lymphatic system. How nanoparticles translocate is not fully understood. Translocation through cells can be active or passive, whereas transport between cells is restricted to nanoparticles that fit in the cell gaps or interact with cell junctions, or occurs during inflammation when junctions are disrupted (Muhlfeld *et al.*, 2008). Another suggested mechanism is transport with the help of macrophages and dendritic cells, especially to the lymphatic system (Harmsen *et al.*, 1985). Interestingly, nanoparticles have been reported to re-enter the lung (Semmler-Behnke *et al.*, 2007). Translocation of nanoparticles into extrapulmonary organs is low in general and, much like intravenously injected nanoparticles, inhaled nanoparticles tend to target the mononuclear phagocyte system (Kermanizadeh *et al.*, 2015; Johanson *et al.*, 2016). However, increased inhaled doses increase transport to lymph nodes (Tran *et al.*, 2000; Keller *et al.*, 2014).

Nanoparticles deposited in the nose region during nasal breathing can be swallowed, sneezed and coughed out. In addition, translocation into the brain via axons in olfactory nerves has been demonstrated (DeLorenzo, 1970; Elder *et al.*, 2006). Olfactory uptake of magnesium oxide nanoparticles resulted in inflammatory changes in the brain (Elder *et al.*, 2006). Size influences deposition and translocation.

2.1.2.3 Dermal exposure

Nanoparticles are applied on the skin intentionally via cosmetics, but also unintentionally via products not designed for skin contact. In textiles, nanoparticles of silver and other metals are added to achieve properties referred to as, *e.g.*, anti-bacterial, water-repellent, UV-absorbing, and wear and tear resistant. Nanoparticles can also be found in products such as motor oil, fuel catalysts and cleaning products, with potential consumer and occupational exposure (Poland *et al.*, 2013).

Skin is a large organ (15% of the body weight) and prevents loss of water and heat as well as protects the body from mechanical, biological and chemical hazards. It consists of three layers; hypodermis, dermis and epidermis (Johanson *et al.*, 2008). The outermost layer of the epidermis, stratum cornea, provides the major barrier for nanoparticle uptake. To get into systemic circulation nanoparticles have to penetrate the stratum cornea, especially via hair follicles, sweet glands or intra/intercellular routes. Passage via hair follicles and sweet glands

is the most probable route for nanoparticles. Intercellular routes are limited to small nanoparticles and intracellular routes are primarily accessible for chemical substances and ions (Johanson *et al.*, 2016).

The permeability of nanoparticles through intact skin is small but several factors may increase the extent of uptake. (Tinkle *et al.*, 2003; Johanson *et al.*, 2008; Filon *et al.*, 2011; Filon *et al.*, 2015) These include anatomical site (skin thickness), skin humidity, temperature, barrier integrity, mechanical flexion, nanoparticle properties, contaminants in nanoparticles, and dissolution of nanoparticles. Wounds, detergents, organic solvents and skin burns may destroy the integrity of the skin and provide breached barrier function to nanoparticles. Dissolution of nanoparticles results in release of chemical substances and ions with increased permeability over nanoparticles (Filon *et al.*, 2015; Midander *et al.*, 2016). With decreased size the probability for uptake increases (Filon *et al.*, 2015; Johanson *et al.*, 2016). Uptake through intact skin has been demonstrated for sizes smaller than 4 nm, and penetration via follicles and sweet glands seems to be possible for sizes up to 20 nm. On the other hand, penetration and permeation of sizes above 45 nm probably only take place in severely damaged skin (Filon *et al.*, 2015).

2.1.2.4 Oral exposure

Oral exposure to nanoparticles may result from ingestion of food, fluids or drugs (Etheridge *et al.*, 2013; McCracken *et al.*, 2016). In addition, exposure can also occur through unintended swallowing of products containing nanoparticles or ingestion of nanoparticles released from products during interactions such as licking, sucking and chewing. Inhaled airborne particles also end up in the gastrointestinal tract when deposited non-respiratory fractions or mucociliary cleared particles are swallowed (Oberdörster, 1988; Snipes, 1989). Systemic uptake via oral exposure is an attractive distribution pathway for nutrients and drugs. Several efforts have been made to improve absorption by modification of size, shape and surface properties (Mei *et al.*, 2013). However, reported absorption differs significantly between studies, where several studies could not demonstrate any uptake and other studies measured uptake of several per cent of administered dose (Johanson *et al.*, 2016).

In the gastrointestinal tract, the nanoparticles interact with the local environment, including food components, which affect the uptake and the toxicity (Cao *et al.*, 2016). During this interaction proteins and biomolecules adhere to the nanoparticle surface forming a corona (Docter *et al.*, 2015). So far, only a few *in vitro* studies have evaluated the impact of the corona on uptake, but the results suggest increased absorption (Di Silvio *et al.*, 2016). Increased absorption and toxicity can also be a result of dissolution of the nanoparticles, as reported for zinc oxide nanoparticles (Wang *et al.*, 2014). On the other hand, nanoparticles can also affect the nutrient uptake by either damaging the intestinal cells or changing the expression in nutrient transporters (Mahler *et al.*, 2012; Dorier *et al.*, 2015).

To enter the body, nanoparticles have to overcome two barriers: the mucus and the epithelium. The first barrier, the mucus, is a sticky, hydrophobic and negatively charged gel wherein nanoparticles can be trapped (Lai *et al.*, 2009). The continuous renewal of mucus transports trapped nanoparticles distally to faeces. If nanoparticles manage to migrate through the mucus, they have to pass the second barrier, the epithelium, to reach the systemic circulation (des Rieux *et al.*, 2006). The dominant cell type in the intestinal epithelium is the enterocyte, but it does not seem to account for the major transcellular transport, though uptake has been demonstrated. Instead, transport takes place in the less numerous M-cells in

the Peyer's patch. M-cells account for approximately 1 % of the intestinal epithelium cell population and are part of the mucus-associated lymphoid tissues. From the interstitial space, nanoparticles can translocate into blood circulation and lymph systems for further distribution to distal organs and tissues (Li *et al.*, 2010; Roger *et al.*, 2010).

2.2 PHYSIOLOGICALLY BASED PHARMACOKINETIC (PBPK) MODELLING

PBPK models provide information about mass-time profiles of individual tissues and organs and use mathematical equations to describe how substances are absorbed, distributed, metabolized and excreted over time (IPCS, 2010; Krishnan *et al.*, 2010; Johanson, 2014). By incorporation of knowledge about anatomy, physiological mechanisms and substance kinetics, the mathematical model can predict the internal dose of a substance based on information about external exposure. PBPK models also allow interspecies extrapolation,where findings from animals can be scaled up to humans without additional testing. In fact, PBPK models are used for drug development, animal toxicity test designs and human health risk assessments. Moreover, PBPK models are useful for extrapolation between species, doses and routes of exposure.

A PBPK model is structured into compartments that represent organs (IPCS, 2010; Krishnan *et al.*, 2010; Johanson, 2014). Each compartment is organized in a biologically relevant position and compartments are interconnected through the mass transport between them. How many the compartments are and how they are structured is determined by the intended use of the model and knowledge about the substance(s) of interest. Typically, the model includes separate compartments for target tissues, tissues with biotransformation and clearance, and storage tissues. To avoid over-parameterization and reduce computation time, the complexity of the model should be minimized. Pooling of organs is one way of doing this, where tissues with similar properties, such as blood flow and partitions, are lumped into a joint compartment.

Substances enter the system by exposure routes such as inhalation, injection into blood, dermal contact and/or digestion. To reach the circulatory system for further transport to distal organs, substances may need to pass barriers. Transport over barriers occurs by active or passive processes. Once absorbed, substances are distributed to organs via the circulatory system. In the organs, substances move into the tissue, a phenomenon often described by mass-balance differential equations of the first order with either perfusion- and or diffusion-limited processes. Distribution between blood and tissue may for substances be described by a partition coefficient, which assumes a well-stirred compartment in a quasi-steady state. Clearance occurs from organs such as the liver and kidney and may involve metabolism. When processes involve saturation they can often be described using Hill equations.

The model includes parameters which are physiologically based or substance-specific and are typically derived from scientific literature, experiments or estimated by the model (IPCS, 2010; Krishnan *et al.*, 2010; Johanson, 2014). Body and organ weight, blood flow, and ventilation rate are examples of physical parameters, whereas partition and metabolic rates are examples of substance-specific parameters.

Optimizing the performance of a PBPK model is an iterative process (IPCS, 2010; Krishnan *et al.*, 2010; Johanson, 2014). The process starts with comparing predictions with experimental data from biodistribution studies and then refining the model, if they do not cohere. Refinements involve adjustment of model structure and/or optimization of parameters

to provide the best fit between predictions and experimental observations. The process is called calibration. During validation, the performance of the calibrated model is evaluated by comparing the model predictions with external data, *i.e.*, data not used for calibration. Model performance is evaluated by visual inspection and/or goodness-of-fit criteria, such as, coefficient of determination (R^2), maximum log-likelihood and the Akaike information criterion.

To identify model parameters that influence model outcome the most, sensitivity analyses are carried out (IPCS, 2010; Krishnan *et al.*, 2010; Johanson, 2014). This is important as a small change in a sensitive parameter will have a large impact on the accuracy of the output. Sensitivity analysis is a quantitative evaluation, where a change in response/output is measured as a result of a change in an input parameter. Changing one parameter at a time is called local sensitivity analysis. Local sensitivity analysis has the limitation that covariates and interactions between parameters cannot be assessed. By varying multiple parameters simultaneously such relationships can be assessed. This is referred to as a global sensitivity analysis. However, a global sensitivity analysis requires a powerful computer processor, which often limits its usability.

2.2.1 PBPK model for intravenously injected nanoparticles

An increasing number of PBPK models for nanoparticles injected intravenously have been published; most of them aim to describe experimental data (Table 1).

Table 1. Summary of PBPK models for rodents injected intravenously with nanoparticles.

Type of nanoparticles	Model parameter			Model evaluation			References
	Partition	Permeability	Phagocytosis	External validation	Sensitivity analysis	Goodness of fit	
PT-ODN	x	x	-	-	-	Visual	(Peng *et al.*, 2001)
Quantum dots	x	-	-	-	[b]	Visual	(Lin *et al.*, 2008)
Quantum dots	x	-	-	x	-	Visual	(Lee *et al.*, 2009b)
Silver	x	-	x[a]	-	-	Visual	(Lankveld *et al.*, 2010)
MINP	x	x	-	x	Local	Visual	(Opitz *et al.*, 2010)
Gold dendrimers	x	x	x[a]	-	Global	Visual	(Mager *et al.*, 2012)
PLGA	x	x	-	-	Local	R^2	(Li *et al.*, 2012)
Silver	x	x	x	x	Local	Visual	(Bachler *et al.*, 2013)
Titanium dioxide	x	x	x	x	Local	Visual	(Bachler *et al.*, 2015b)
PAA	x	x	x	-	Local	R^2	(Li *et al.*, 2014)
Gold	x	x	x	x	Local	R^2	(Lin *et al.*, 2015a)
Block co-polymer	x	-	-	-	Local	Visual	(Gilkey *et al.*, 2015)
Titanium dioxide	x	-	-	-	-	AIC + BIC	(Elgrabli *et al.*, 2015)
Zinc oxide	x	-	-	-	Local	MAPE	(Chen *et al.*, 2015)
Gold	x	x	x	x	-	R^2	(Lin *et al.*, 2016)
Gold, titanium dioxide, PAA, PAA-PEG	x	x	x	-	Local	R^2, PBPK indices	(Carlander *et al.*, 2016)

[a] Uptake to a storage compartment in tissue

[b] Performed but no details provided

Abbreviations: AIC - Akaike information criterion, BIC - Bayesian information criterion, MAPE - mean absolute percentage error, MINP – Magnetic imaging nanoparticles, PAA – Polyacrylamide, PLGA - poly(lactic-co-glycolic acid), PT-ODN - phosphorothioate oligonucleotide, R^2 - coefficient of correlation.

The early models followed the structure used for xenobiotics, but they did not adequately explain the more complex kinetics exhibited by nanoparticles. To improve the models, additional factors of relevance for nanoparticles have been incorporated, such as phagocytosis and permeability restrictions (Peng *et al.*, 2001; Li *et al.*, 2014). Time- and size-dependent phagocytic rates and time-dependent partitioning are other examples of modifications implemented into PBPK models for nanoparticles (Lin *et al.*, 2008; Bachler *et al.*, 2013; Chen *et al.*, 2015; Lin *et al.*, 2015a). Evaluation of the performance of models has frequently been done by visual inspection, but statistical methods such as coefficient of correlation and the Akaike criterion have also been used. Validations of models with external data and to additional species have not always been performed, which probably reflects the lack of suitable data for modelling. So far, most models are limited to a single type of nanoparticles and models for repeated and life-long exposure are not yet available.

2.2.2 PBPK model for inhalation of nanoparticles

The number of published PBPK models for inhaled nanoparticles is limited and their usability is restricted to a few types of nanoparticles, see Table 2. The structure differs widely between the models, for example as regards the structure of the lung and the number of extra pulmonary organs. The respiratory system is described by one or several compartments and some models include alveolar macrophages. In the lung, the majority of the nanoparticles are cleared via uptake by alveolar macrophages and mucociliary clearance, described in models with separate transport processes or as a joint process. From the lung, a fraction of deposited nanoparticles is transported to the interstitium, lymph system and/or blood circulation. In addition, some models address uptake to the brain via the olfactory system. When nanoparticles are cleared from the lung via mucociliary clearance the majority of the models assume that nanoparticles reach the gastrointestinal tract and/or get cleared by cough or sneezing.

Table 2. Summary of PBPK models for inhalation of nanoparticles and compartments included in the model structure.

Type of nanoparticles	Number of compartments in		Compartments in model					References
	Extra pulmonary organs[a]	Breathing system[b]	Olfactory	Lymph	AM	PC	GIT	
Aluminium silicate	3	4	-	x	-	-	x	(Snipes *et al.*, 1983)
Iridium	9	6	x	x	x	x[c]	x	(MacCalman *et al.*, 2009)
Carbon	22	2	-	-	-	-	x	(Pery *et al.*, 2009)
Ag, Au, QD, PS, carbon	11	2	-	x	-	-	x	(Li *et al.*, 2011)
Iridium, Co_3O_4, Tb_2O_3	4	12	x	x	x	-	-	(Kolanjiyil *et al.*, 2013)
Ag	10	1	-	-	-	x	x	(Bachler *et al.*, 2013)
Gold	6	2	-	-	X[d]	-	-	(Bachler *et al.*, 2015a)
Iridium and silver	10	6	x	x	x	x[c]	x	(Sweeney *et al.*, 2015)
Nanoceria	10	7	x	-	x	x	x	(Carlander *et al.*, 2016)

[a] All organs and tissues outside the breathing system

[b] Compartments for deposition as upper respiratory tract, tracheobronchial region, alveolar region and sub-compartments such as AM, lung interstitium and lung lymph nodes

[c] Uptake to a storage compartment in tissue

[d] Not expressed as uptake to AM, but similar to uptake to AM

Abbreviations: Ag - silver, AM - alveolar macrophages, Co_3O_4 - cobolt oxide, GIT - gastrointestinal tract, PS - polystyrene, QD - quantum dots, Tb_2O_3 - terbium oxide

Building a PBPK model for inhalation information regarding deposition in the lung is essential. To get information about deposition in the respiratory system, deposition models and/or experimental data are used. Several computational models and approaches are available to describe and calculate deposition of particles in the lung (Hofmann, 2011). Deposition models can be divided into two categories depending on the intended use: whole-lung or local deposition models. The whole-lung model provides information about deposition in the entire respiratory system, whereas the more complex and computer-intense local models so far only address local deposition in the upper respiratory tract. In PBPK modelling, whole-lung deposition models are more frequently used than local deposition models and the most commonly used model is probably the Multi-Path Particle Dosimetry (MPPD) model (Anjilvel *et al.*, 1995; RIVM, 2002).

The MPPD model is an open access software that calculates deposition and clearance of mono-dispersed and poly-dispersed particles in the range 0.01 µm to 2 µm in the respiratory system of humans and animal species such as rats, mice, rabbits and pigs. A fraction of the particles from external exposure are filtrated in the nose and mouth, described by an empirical efficiency function in the model. Once inhaled, particles will be deposited and the deposition is theoretically calculated by diffusion, sedimentation and impaction, calibrated and validated with external data. The structure of the lung is represented either by a single symmetric tree or by a multi-path branching, as selected by the user. The asymmetric branching pattern of the multi-path model has been derived from actual measurements on lung casts. To receive information about deposition and clearance, the model requires input data from the user on a breathing scenario and particle properties. The output presents calculations on total, regional (head, tracheobronchial, and pulmonary) and lobar fractional deposition. Regional deposition values from the MPPD model have been used as input for PBPK models, but the MPPD model has not yet been incorporated as part of the model.

2.2.3 PBPK model for mixed exposure routes

Only three PBPK models for mixed exposure routes to nanoparticles have been published so far (Li *et al.*, 2011; Bachler *et al.*, 2013; Bachler *et al.*, 2015b). These models include inhalation, dermal contact and/or digestion of nanoparticles.

One of the models is framed as a general PBPK model and covers inhalation, digestion and intravenous injection of different types of nanoparticles and species (Li *et al.*, 2011). To predict biokinetics, first-order mass transfer rates to and from organs in well-mixed compartments are used, but the model does not account for, *e.g.*, diffusion-limited processes, phagocytosis, degradation or size-dependent deposition in the lung. Pooled data from *in vivo* studies on various types of nanoparticles and exposure conditions and routes have been used for calibration.

The other two models have similar model structures; one is designed for silver ions and silver nanoparticles (15 nm to 150 nm) and the second describes the biokinetics of titanium dioxide nanoparticles (Bachler *et al.*, 2013; Bachler *et al.*, 2015b). Both models include the same organs, use permeability-restricted transport processes and allow uptake of nanoparticles directly from blood to phagocytes in liver, spleen and lung. In addition, both models use first-order mass transfer rates and have been optimized with rodent and human biokinetic data. On the other hand, they differ in that the silver model has a substructure for ions and a size-dependent uptake rate in phagocytic cells, which the titanium dioxide model does not.

In short, all three models are reported to perform well, but as no clear relationships between nanoparticle properties, exposure conditions and model parameters are provided their usability for risk assessment is limited. Consequently, extrapolations between nanoparticle types, species, doses and routes of exposure are not yet possible.

2.2.4 Dissolution in PBPK modelling

So far, only one PBPK model for nanoparticles includes dissolution. This models describes the biokintics for silver nanoparticles and the dissolution of silver into silver ions and glutathione bounded silver (Bachler *et al.*, 2013).

Dissolution is a process that makes metallic nanoparticles transform into ionic species and by which their properties and abundance are altered. The dissolution rate and characteristics of dissolved species depend on the characteristics of the nanoparticles, such as chemical composition, size, shape, crystallinity, surface coatings and agglomeration, as well as on the surrounding media and exposure conditions, such as dose, composition, ion strength, pH, and temperature (Costa *et al.*, 2001; Mishra *et al.*, 2011; Utembe *et al.*, 2015; Feliu *et al.*, 2016a). If the dissolution rate is low, the risk for bioaccumulation increases, but if the dissolution rate is high, substances can migrate and dissolve into surrounding media. Dissolved and solubilized substances can, in fact, have different properties, toxicity and biokinetics compared with the nanoparticles, and consequently requires consideration in PBPK modelling (Molina *et al.*, 2014; Sabella *et al.*, 2014).

Dissolution of metals involves release of ions. Some ions complex bind to substances in the surrounding environment, which sometimes results in generation of new types of nanoparticles as observed for silver and cerium (Loeschner *et al.*, 2011; van der Zande *et al.*, 2012; Graham *et al.*, 2014). Consequently, the abundance in tissue can be a mixture of nanoparticles, complex bounded ions, and free ions, making analysis challenging and the biokinetics complex.

Inclusion of dissolution in PBPK models requires experimental data on the biokinetics of nanoparticles as well as on the dissolved species. However, most biodistribution studies performed on metallic nanoparticles have only used elementary analysis such as ICP-MS and atomic absorption spectroscopy to measure the organ burden, and hence cannot distinguish between different forms of metals (Johanson *et al.*, 2016).

Modelling dissolution kinetics of nanoparticles is under development but such models have not yet been implemented in PBPK models for nanoparticles (Costa *et al.*, 2001; Mishra *et al.*, 2011; Utembe *et al.*, 2015). These dissolution models are often based on experience from larger particles and assume release from surfaces. To describe dissolution mathematically, zero-, first-, or second-order kinetics with release rate constants dependent on surface area, volume and diffusion have been tested. The majority of existing models for nanoparticles are related to particles with high dissolution rates and *in vitro* conditions.

3 AIMS

The PBPK simulations were performed assuming that the nanoparticles are inert, *i.e.* do not dissolve or degrade in the body. When modelling the experimental data it seemed that the biokinetics might be better explained by introducing dissolution in the PBPK model. Therefore, an additional aim was introduced, *i.e.* to evaluate dissolution of stable nanoparticles in the presence of macrophages.

The specific aims were:

1. To develop and verify a PBPK model for stable nanoparticles that were administered intravenously (Papers I, II and III).
2. To extend the PBPK model to account for other routes of exposures (Papers III and IV).
3. To evaluate the stability of gold nanoparticles when exposed to macrophages (Paper V).

4 MATERIALS AND METHODS

This section summarizes the materials and methods used for this thesis (Papers I-V). The first part relates to the development of nano PBPK models and presents how the PBPK model was evaluated and modified to describe biokinetics of nanoparticles considered inert, such as polyacrylamide (PAA), gold (Au), titanium dioxide (TiO_2) and cerium dioxide (nanoceria and CeO_2) when delivered to rats via intravenous administration, inhalation, instillation and ingestion (Papers I-IV). The second part describes a follow-up study from a finding in Paper II related to the dissolution of gold by macrophages (Paper V).

4.1 PBPK MODELLING OF NANOPARTICLES

The process used to develop PBPK models for nanoparticles considered inert and administered intravenously or via inhalation, instillation and ingestion into rats is described in Figure 2 and summarized in paragraphs 4.1.1 to 4.1.5. More detailed information can be found in Papers I-IV.

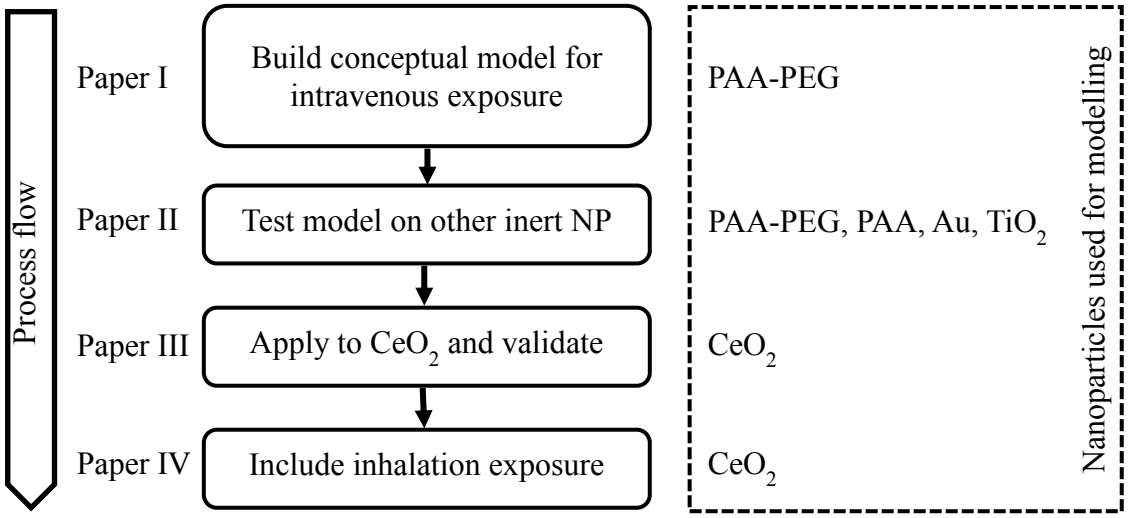

Figure 2. Overview of the modelling process in this thesis.

4.1.1 Development of a nano PBPK model for intravenous exposure

As a first step a PBPK model for nanoparticles injected intravenously into rats was developed (Paper I). Conceptually, the model represents systemic exposure without involvement of absorption barriers. The model was designed based on experimental data on tissues/organs and body fluids analysed for polyethylene glycol-coated polyacrylamide (PAA-PEG) nanoparticles, combined with general information about the biokinetic behaviour of nanoparticles.

To build a conceptual PBPK model for inert nanoparticles injected intravenously, experimental data from a published study on PAA-PEG was used (Wenger *et al.*, 2011). The PAA-PEG study was designed for PBPK modelling and hence contained relevant data, *i.e.*, data from multiple organs, multiple post-injection follow-up times, and total recovery, see Table 4. The PAA-PEG nanoparticles were administered with a bolus intravenous dose to

five groups of rats. Organs were collected and analysed with liquid scintillation counting of C^{14}.

The model contains ten compartments: arterial and venous blood, liver, spleen, lung, kidney, heart, brain, bone marrow and other organs. The lymphatic system was not included in the model, even though data was available and this probably is a common pathway for nanoparticles. However, adding the lymph system to the model would introduce increased model complexity. In addition, model optimization had to be carried out on values that contributed to a negligible amount of the total body burden (< 0.1 %).

Each organ compartment is subdivided into three sub-compartments: capillary blood, tissue and phagocytic cells, with venous and arterial blood described by two sub-compartments: blood and phagocytic cells. The compartments are interconnected with each other via blood flow and organized in physiological order. Excretion to faeces takes place from liver tissue and to urine from capillary blood via the kidneys.

The model parameters consist of nanoparticle-independent parameters and nanoparticle-dependent parameters, summarized in Table 3. Values on physiological parameters were primarily taken from experiments and secondarily collected from the literature (Brookes, 1967; Bernareggi *et al.*, 1991; Brown *et al.*, 1997; Travlos, 2006). Data on the nanoparticle uptake capacity of phagocytic cells in organs were sparse and therefore experimental data were used as a basis for model estimation of these parameters. All nanoparticle-dependent parameters were fitted.

Table 3. Summary of model parameters in PBPK model for intravenous administration of nanoparticles.

Nanoparticle-independent	Nanoparticle-dependent parameters
• Bodyweight • Cardiac output • Fraction of cardiac output to tissue/organ • Fraction of total bodyweight for different tissues • Fraction of blood in different tissues • Fraction of residual blood in brain • Fraction of residual blood in tissue	• Rate of clearance in urine (CL_u) • Rate of clearance in faeces (CL_f) • Rate of uptake by phagocytic cells (K_{ab0}) • Rate of uptake by phagocytic cells in spleen (K_{sab0}) • Uptake capacity of phagocytic cells in different tissues ($M_{cap,i}$) • Tissue:blood partition coefficient (P) • Coefficient of permeability from blood to the liver, spleen, lung, kidney, heart and brain (X_{fast}) • Coefficient of permeability from blood to other organs (X_{rest}) • Coefficient of permeability from blood to the brain (X_{brain})

The transport of nanoparticles from blood to tissues/organs is described by flow- and diffusion-limited processes, and in the PBPK model controlled by the coefficients for permeability and fractions of cardiac output to organs. There are three permeability coefficients in the model. The first is used for fast perfused organs (X_{fast}): liver, spleen, lung, kidney, heart, and bone marrow, while the second is designed for brain (X_{brain}) and the third is utilized for other organs (X_{rest}). The permeability coefficient in brain is set to zero, based on the assumption of a tight and impermeable blood-brain barrier.

During the development of the model, inclusion of a tissue:blood partition coefficient in the PBPK model was needed to describe the biokinetics of PAA-PEG nanoparticles. This is assumed to reflect the changes in the corona formed on the particles due to differences in composition of blood and interstitial fluid, causing PAA-PEG to have a preference for blood over tissue (Lundqvist *et al.*, 2008; Monopoli *et al.*, 2012). Despite differences in composition of interstitial fluids between tissues, the tissue:blood coefficient kept the same value for all organs/tissues.

In tissue, the phagocytic cells engulf a fraction of the nanoparticles and eventually the phagocytic cells get saturated. The saturation process is controlled by the balance between uptake and exocytosis rates and the maximum uptake capacity of phagocytic cells in tissues. The uptake rate is described as a function of maximum uptake capacity and decreases as the phagocytic cells reach saturation. Moreover, the maximum uptake capacity in each organ is assumed to reflect the density of phagocytic cells in tissue.

According to the study design for PAA-PEG, the blood vessels were not rinsed before harvesting of organs (Wenger *et al.*, 2011). Consequently, residual blood may have remained in organs. In fact, the levels in brain could be explained by implementation of a coefficient that assumes that the capillary blood in organs was not entirely removed when organs were harvested. In the model, two coefficients accounting for fraction of residual bloods in organs were introduced and fitted to observed data, one constant for the brain and another constant for all other organs.

4.1.2 Expansion of the PBPK model to other nanoparticles given intravenously

As a next step, the model was expanded to other inert nanoparticles (Paper II).

Data for modelling were retrieved from the literature to evaluate if the model in Paper I could describe the biokinetics of other considerable inert nanoparticles intravenously injected in rats. To find such data, a literature review was carried out in SciFinder, PubMed, Google Scholar and Web of Science and reference lists in papers were scrutinized. Information about nanoparticle properties, study designs and test results were extracted from the collected studies (> 200 data sets). To select data sets for modelling, the following criteria were used:

1. The nanoparticle and its label should not be soluble or degradable.
2. The dose should be reported in quantitative units.
3. The amount or concentration in organs should be reported or possible to extract from figures in quantitative units.
4. The organs analyzed should include blood, liver, spleen and at least two additional organs or tissues.
5. The observation period post-injection should be at least 24 h, with at least four sampling times.
6. The total recovery in all reported tissues/organs monitored must be at least 25 % of the injected dose.

Using the above criteria, three data sets on polyacrylamide, gold and titanium dioxide nanoparticles were found, in addition to the data set in Paper I. Numerical data were reported in the papers for coated and uncoated polyacrylamide and for titanium dioxide, but data on gold had to be extracted from figures and the bodyweight estimated based on the strain and

age of rats used. Study characteristics of the four data sets in Paper I and Paper II are summarized in Table 4.

The model structure is the same as in Paper I, but the model parameter describing uptake capacity in phagocytic cells in tissues (M_{cap}) has been modified and the grouping of organs correlated to the three blood-organ coefficients of permeability (X_{fast}, X_{rest} and X_{brain}) were elaborated.

In Paper I, it was assumed that all phagocytic cells behaved the same but that their abundance varied between organs. The parameter (M_{cap}) was defined as the uptake capacity of phagocytic cells per gram tissue and hence independent (number of phagocytic cells per gram tissue) and dependent (uptake capacity of an individual phagocytic cell) of nanoparticle properties. To separate the nanoparticle-dependent part from (M_{cap}), (M_{cap}) was divided into two coefficients in Paper II. The first coefficient described the number of phagocytic cells per gram tissue ($N_{cap,\ tissue}$) and the second described the uptake capacity of an individual phagocytic cell (M_{capPC}). This separation made it possible to compare uptake capacity of phagocytic cells predicted by the model with experimental data from *in vitro* studies.

There are three blood-organ coefficients of permeability in the PBPK model. Each coefficient is connected to a set of organs. The grouping of organs was elaborated to explore dependence on permeability in endothelium and presence of phagocytic cells in direct contact with blood. Three different groupings were tested. The first grouping was the same as in Paper I. In the second, the (X_{fast}) was assigned to spleen and liver. In the third, the (X_{fast}) was reserved for liver, spleen and bone marrow.

Table 4. Summary characteristics of data sets for nanoparticles intravenously administered to rats, used to develop the nanospecific PBPK model in Paper I, Paper II and Paper III.

Material	***PAA***	***PAA***	***Gold***	***TiO_2***	***CeO_2***	***CeO_2***	***CeO_2***
Trade name	Synthesized	Synthesized	Synthesized	Degussa P25	Synthesized	Synthesized	Synthesized
Coating	PEG	No	CTAB	No	Citrate	Citrate	Citrate
Shape	Sphere	Sphere	Rod	Sphere	Polyhedral	Polyhedral	Cubic
Size (nm)	D:31	D:31	L:56 D:13	D:63	D:5	D:5	D:30
Size method	DLS	DLS	TEM	DLS	TEM	TEM	TEM
Z-potential (mV)	+2.3	-	+29	-43	-53	-53	-56
Dose (mg/kg)	28	45	0.56	0.95	85	11	85
Dosing	Bolus	Bolus	Bolus	Bolus	1 h infusion	1 h infusion	1 h infusion
Sampling times, post dosing (h)	0.08, 0.17, 0.5, 1, 4, 8, 24, 48, 72, 96, 120	0.08, 0.17, 0.33, 0.67, 1, 2, 4, 8, 24, 72, 96, 120	0.5, 1, 4, 16, 24, 72, 168, 336, 672	6, 24, 72, 168, 720	1, 20, 720		1, 20, 720, 2160
Rat strain	Sprague Dawley	Sprague Dawley	Sprague Dawley	F344/DuCrlCrlj	Sprague Dawley	Sprague Dawley	Sprague Dawley
Bodyweight (g)*	253	253	160 [a]	244	425	440	441
Number of animals	2-3	2-3	3	5	7-12	5	3-7
Organs collected	Bl, Li, Sp, Lu, Ki, He, Br, Lymp, BM, Carcass	Bl, Li, Sp, Lu, Ki, He, Br, Lymp, BM, Carcass	Bl, Li, Sp, Lu, Ki, He, Br, Bo, Mu	Bl, Li, Sp, Lu, Ki, He, Br, Lymp	Bl, Li, Sp, Br	Ad, Bl, BM, Bo, Br, Fa, He, Ki, Li, Lu, Mu, Sk, Sp, Te, Ty	Ad, Bl, BM, Bo, Br, He, In, Ki, Li, Lu, Mu, SF, Sk, Sp, Te, Ty
Excretion	U+F	U+F	U+F	U+F	-	-	U+F
Analytical method	C14	C14	ICP-MS	ICP-SFMS	ICP-MS	ICP-MS	ICP-MS
Paper(s)	I	I+II	II	II	III	III	III
Reference	Wenger 2011	Wenger 2011	Wang 2010	Shinohara2014	Yokel 2013	Yokel 2014	Yokel 2012

[a] Bodyweight used in model

Abbreviations: Ad – adrenal gland, Bl - blood, BM - bone marrow, Bo - bone, Br - Brain, C^{14} - carbon-14 radioactivity, CTAB - cetyltrimethylammonium bromide, D – Diameter, DLS – Dynamic Light Scattering, Fa – fat, F – Faeces, He - heart, ICP – Inductively Coupled Plasma, In - intestine, Ki - kidney, L – Length, Li - liver, Lu - lung, Lymp - lymph nodes, MS – Mass Spectroscopy, Mu - Muscle, PAA - polyacrylamide, PEG - polyethylene glycol, SF-spinal fluid, SFMS - Sector Field Mass Spectroscopy, Sk – Skin, Sp - spleen, Te – Testis, TEM – transmission electron microscopy, TiO_2 - titanium dioxide, Ty – Thymus, U – Urine.

4.1.3 Expansion of the PBPK model to nanoceria administered by various routes

Next, biokinetics for cerium dioxide nanoparticles (CeO_2 or nanoceria) were characterized using the same model structure as in Paper II, but also modified to include inhalation, instillation and oral exposure (Paper III).

Raw data were received from Yokel and colleagues on nanoceria infused intravenously into rats and additional biodistribution studies on intravenous, inhalation, instillation and oral exposure were collected from the literature. A literature review was performed using SciFinder, PubMed, Google Scholar and Web of Science and scrutinizing reference lists in papers. If data were presented as figures, data was extracted using WebPlotDigitizer version 2.6. In total, we found 16 data sets from eight studies for intravenous exposure covering different sizes (3, 5, 15, 30, 40 and 55 nm), coatings (uncoated, citrate, citrate/EDTA coated), doses (between 6 and 750 mg/kg) and dosing methods (bolus and infusion) (Yokel *et al.*, 2009; Hardas *et al.*, 2010; Dan *et al.*, 2012; Yokel *et al.*, 2012; Heckman *et al.*, 2013; Yokel *et al.*, 2013b; Yokel *et al.*, 2014; Konduru *et al.*, 2016). The number of inhalation and instillation studies was seven, including 16 data sets (He *et al.*, 2010; Nalabotu *et al.*, 2011; Geraets *et al.*, 2012; Keller *et al.*, 2014; Molina *et al.*, 2014; Konduru *et al.*, 2015b; Konduru *et al.*, 2016; Li *et al.*, 2016). Ingestion of nanoceria was described in four studies, covering nine data sets (Park *et al.*, 2009; Kumari *et al.*, 2014a; Kumari *et al.*, 2014b; Molina *et al.*, 2014). For more information about collected studies, see Paper III.

The richest data set/sets (most organs and at least three sampling times post-administration) among the biodistribution studies for intravenous administration were selected and used for optimization of PBPK models to experimental data on 5 and 30 nm nanoceria. To meet criteria on multiple organs and frequent sampling, two studies had to be used for optimization of PBPK model to 5 nm nanoceria (Yokel *et al.*, 2013b; Yokel *et al.*, 2014). For optimization of the model to 30 nm nanoceria, the richest data set, reported by Yokel and colleagues in 2012, was employed (Yokel *et al.*, 2012). The remaining data sets were utilized for validation of the model: four data sets for the 5 nm PBPK model and five for the 30 nm PBPK model. A summary of study characteristics for the three data sets used for optimization in Paper III is presented in Table 4. Data on 15 and 50 nm did not have sufficient information for model calibration, instead they were compared with predictions from the PBPK model calibrated to 5 nm and 30 nm nanoceria.

In addition to the work done in Paper II, the model's predictability for independent data sets was evaluated (validation), as such data were available. The model was the same as in Paper II, but nanoparticle-dependent parameter in the model were re-optimized separately for 5 and 30 nm nanoceria. We also tested two other models from other research groups, Lin and Bachler and their colleagues, but the outcomes from these models are not reported as they did not improve the results (Bachler *et al.*, 2015b; Lin *et al.*, 2016).

The impact of exposure routes on biokinetics was compared with that of intravenous administration, by calculating and comparing the ratios between reported concentration in internal tissues/organs and the concentration in liver. To study differences in absorption efficiency, the mass ratios between liver and lung or liver and administered dose were calculated and compared for inhalation, instillation and oral data.

To simulate uptake into the circulatory system after oral and lung exposure, the PBPK model was modified by adding compartments for such exposure routes: one compartment for uptake from lung and one compartment for absorption from gastrointestinal tract. Absorption into systemic circulation was described by first-order kinetics. Clearance via the mucociliary escalator in lung and clearance to faeces in the gastrointestinal tract were expressed using first-order clearance rates. The clearance rate constants and the absorption rate constants in the modified model were estimated by fitting the constants, one by one, to each individual data set collected for inhalation, instillation and oral exposure. All other parameters of the model were kept the same as for the 5 nm PBPK model, but scaled to bodyweight in experiments.

4.1.4 Further refinement of the PBPK model to account for inhalation exposure

Inhalation of nanoparticles results in deposition of nanoparticles in the respiratory system, with potential uptake into the body. In Paper IV, we modified the PBPK model from Paper II to include this type of exposure route by including deposition in the respiratory system and transfer to the GI tract.

Biodistribution data on nanoceria were produced and reported in Paper IV. A experimental system was developed to generate aged and pristine nanoceria and deliver the particles to the respiratory system. Aging involved exposure to ambient urban air conditions with UV light irradiation.

Via a nose-only exposure chamber, Sprague Dawley rats were exposed to combustion-generated nanoceria particles, aged and pristine, during 4 hours. Organs were harvested 15 min, 24 h, and 7 days post-exposure and urine and faeces were collected for the first 24 hours.

In the PBPK model, the respiratory system is divided into three compartments; 1) upper respiratory tract, 2) tracheobronchial region, and 3) pulmonary region. Absorption from the respiratory system into lung tissue is assumed to take place in the pulmonary region following first-order kinetics. In the pulmonary region, alveolar macrophages can engulf deposited nanoparticles. The alveolar macrophages move the nanoparticles to the tracheobronchial region for clearance to mouth via the mucociliary escalator followed by swallowing into gastrointestinal tract. Alveolar macrophages were assumed to behave the same as other phagocytic cells in the model. Transport of alveolar macrophages to tracheobronchial region and clearance via the mucociliary escalator were described by first-order kinetics.

Deposition of nanoparticles in the upper respiratory tract may result in translocation of nanoparticles into the brain via olfactory and trigeminal nerves. Therefore, a first-order uptake rate into brain was included in the model. In addition, deposition of nanoparticles in the upper respiratory tract also results in swallowing into the gastrointestinal tract. In the gastrointestinal tract, uptake into the body can take place and was described by a first-order kinetics in the model.

4.1.5 Computer software and numerical algorithms

All models in Papers I-IV were built in Berkeley Madonna™ version 8.3.18 (Berkeley, CA) and acslX™ Libero version 3.0.2.1 (Huntsville, AL). Berkeley Madonna was used for sensitivity analysis and acslX for optimization.

To solve differential equations, different algorithms were used. Runge Kutta 4 was used for sensitivity analyses, because this algorithm has fixed step sizes. Fixed steps are required when predictions at exact time points are to be compared. On the other hand,nanoparticles covered in this thesis had biokinetic profiles that shifted between fast and slow processes, for such mixed processes Runge Kutta is too slow for optimization and here algorithms using variable step sizes are preferred, such as Gear and CVODE. Gear was used in Papers I and III and CVODE in Papers II and IV.

Optimization was performed in asclX Libero using maximum log-likelihood estimation and Nedler Mead methods. Different algorithms and heteroscedasticities were tested, but in general Nedler Mead tended to give the best maximum log-likelihood values and varying heteroscedasticities had only minor impact on the results. To evaluate results from complex systems, such as PBPK modelling of nanoparticles, there are no general best methods to use and as a result the evaluation methods vary among research groups, see Table 1. In this thesis, the results were evaluated by determining the deviation from the line of unity between the $\log_{10}$ of observed and predicted values and calculating the corresponding R^2. In Paper II, we also used the PBPK indices. In Paper IV, the predictability of the 5 nm PBPK model for nanoceria was evaluated using independent data sets. If the predicted values were within a factor 2 of the observed mean values, the model was considered to be adequately validated, a requirement proposed by the International Programme on Chemical Safety (IPCS, 2010).

To identify model parameters that influence model outcomes the most, sensitivity analyses were carried out using normalized (relative) sensitivity coefficients. These sensitivity coefficients were calculated as the relative change in area under the mass-time curve divided by a change in parameter values.

4.2 DISSOLUTION OF GOLD NANOPARTICLES

An observation we made in Paper II was that the model did not capture the slow decrease in organs with low concentration of gold and titanium dioxide *e.g.* heart and kidney, which may be due to dissolution. If dissolution takes place, contrary to our PBPK model assumption, this will not only influence the biokinetics but also how PBPK models are designed and how toxicological findings should be interpreted. Nanoparticles are taken up by macrophages. Macrophages have the ability to release reactive oxygen species, which may dissolve apparently inert nanoparticles.

To study this, we developed an *in vitro* method and evaluated dissolution of gold in cell medium, cell medium with macrophages or cell medium with macrophages triggered with LPS. This section provides an overview of this dissolution study.

4.2.1 Material – Gold nanoparticles

The dissolution study was carried out using citrated gold nanoparticles from Nanocomposix with diameters of 5 and 50 nm. Gold ions (from $HAuCl_4$) were used to measure recovery of gold ions in the test system.

4.2.2 **Method**

We investigated the dissolution of 5 nm and 50 nm gold nanoparticles at simulated healthy and diseased conditions, *i.e.*, in macrophages and in LPS-triggered macrophages, as well as in cell medium only. Gold nanoparticles were incubated in cell medium (5 µg/ml), with or without murine macrophages (RAW 264.7), for different time periods (0, 24 or 168 h).

After exposure, cell medium and mechanically lysed cells were collected and centrifuged. In practice, the separation of small gold nanoparticles and dissolved gold ions/complexes constituted the crucial experimental challenge. The centrifugation efficiency was improved by the presence of mechanically lysed cells. To allow a direct comparison between the dissolution of gold nanoparticles in media (only) and in media with macrophages, cell lysate was also added to samples of media-incubated gold nanoparticles. By this simple, yet novel, procedure for handling critical separation of small gold nanoparticles and the dissolved fraction we ensured similar test conditions and avoided flaws in the comparison due to different centrifugation efficiencies.

After centrifugation, the supernatant was collected, treated with aqua regia and analysed with inductively coupled plasma mass spectrometry (ICP-MS), to obtain quantitative results of gold dissolution after different time periods. The effect on gold nanoparticle dissolution and relationships between particle size, time of incubation and exposure conditions were evaluated using median linear regression modelling with correlation between all parameters. The dissolution method is summarized in Figure 3.

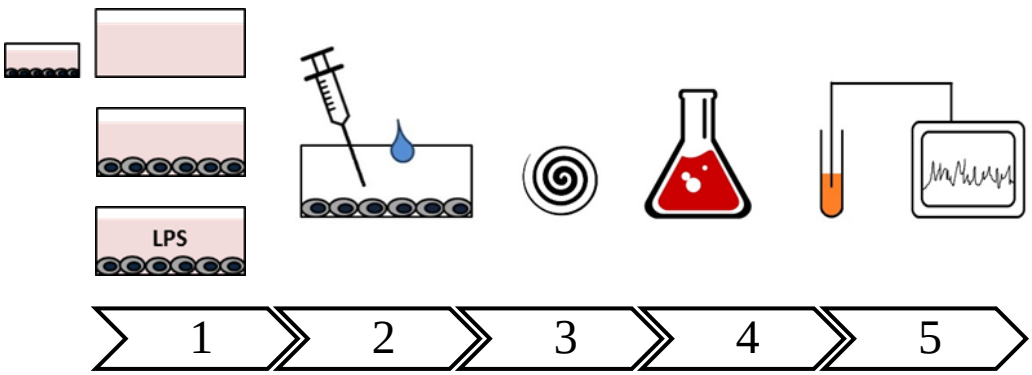

Figure 3. Overview of the method for dissolution of gold nanoparticles in vitro. Step 1: 5 µg of 5 or 50 nm gold particles or 0.25, 1 or 5 µg of Au^{3+} (from $HAuCl_4$) were added to wells with cell medium, macrophages or macrophages triggered with LPS and incubated for 0, 24, or 168 h. Step 2: Cell medium was collected in e-tube. Water was added and the cells were mechanically lysed with a needle and a syringe. Lysed cells were transferred to e-tube with collected cell medium. Step 3: E-tubes were centrifuged for 30 minutes at 13,000 rpm. Step 4: The supernatant was collected and treated with aqua regia for at least 24 hours. Step 5: Aqua regia solution was diluted and internal standards were added, followed by ICP-MS analysis.

5 RESULTS AND DISCUSSION

This section summarizes the results and the discussions for Papers I-V. The first part relates to the development of nano PBPK models for nanoparticles considered inert, delivered to rats via intravenous administration, inhalation, instillation and ingestion (Papers I-IV). The second part describes a follow-up study from a finding in Paper II related to the dissolution of gold by macrophages (Paper V).

5.1 PBPK MODELLING OF NANOPARTICLES

5.1.1 Development of a nano PBPK model for intravenous exposure

As a first step, a conceptual model for inert nanoparticles injected intravenously in rats was developed using polyethylene glycol-coated polyacrylamide (PAA-PEG) nanoparticles as the modelling substance (Paper I). The model accurately described the biokinetics of measured amounts of PAA-PEG in different organs (R^2 on the log scale 0.97).

According to the model, there was a fast initial clearance from blood because nanoparticles were rapidly distributed to organs, where phagocytic cells internalized them until these phagocytic cells became saturated. After four hours, phagocytic cells in most organs were saturated and free nanoparticles were distributed to the rest of the body. Phagocytic cells worked as a storage compartment for nanoparticles. In short, inclusion of a separate compartment for phagocytic cells was successful and a natural component of a PBPK model for nanoparticles.

The sensitivity analysis indicated that the key determinants for the biokinetics of PAA-PEG nanoparticles are the uptake capacities of phagocytizing cells in organs, the partitioning between tissue and blood, and the permeability between capillary blood and tissues.

5.1.1.1 Model structures and parameters

Our model structure for intravenous exposure in Paper I, also used in Papers II-IV with modifications, has some similarities, but also differences, compared with published nano PBPK models, see Table 1. Differences are not only limited to which species and nanoparticles the models have been applied to, but also encompass how many compartments and parameters are included in each model, and how the models were evaluated. Consequently, results from one model cannot readily be compared with results from another, unless the models are applied to the same data sets; this has not been done yet, but would constitute an interesting next step.

Since the publication of Paper I, the concept of phagocytic cells has been implemented in other models, but not necessarily in a similar way as in our model (Bachler *et al.*, 2013; Bachler *et al.*, 2015b; Lin *et al.*, 2015a; Lin *et al.*, 2016). The models by Lin and colleagues assume that the uptake of gold nanoparticles by phagocytic cells occurs directly from blood for larger gold nanoparticles (100 nm), whereas for smaller gold nanoparticles (10 nm) the uptake takes place in the tissue. To describe the uptake rate constant for phagocytic cells, they employed a time-dependent Hill equation, which introduced a more complex model structure with more parameters. In the first model from 2015, Lin and colleagues did not include saturation of phagocytic cells, but in a model reported by the same group in 2016 saturation was added and described as in Paper I (Lin *et al.*, 2015a; Lin *et al.*, 2016). Bachler and co-

workers assumed that the uptake of titanium dioxide by phagocytic cells takes place directly from blood, and can be described by a one-compartment structure without saturation (Bachler *et al.*, 2015b).

Our model assumption is that phagocytic cells behave the same, but their densities in tissue vary (Papers I-IV). In reality, phagocytic cells are diverse and differ across organs, species and conditions of health (Gordon *et al.*, 2005). The large variability obtained from the parameterization of the model coheres with the expected densities of phagocytic cells in tissues. We noticed the highest uptake capacity in organs such as spleen, liver and bone marrow, which is in line with other studies (Lang *et al.*, 1992; Hyafil *et al.*, 2007).

Another simplification we made was to assume a single mechanism for phagocytosis, when in fact multiple endocytotic pathways exist (Sahay *et al.*, 2010; Canton *et al.*, 2012). Endocytosis has also been shown *in vitro* to be highly dependent on the properties of the nanoparticles as well as agglomeration and the corona formation (Chithrani *et al.*, 2006; Jiang *et al.*, 2008; Luciani *et al.*, 2009; Albanese *et al.*, 2011; Lesniak *et al.*, 2012). In our model, the phagocytic process is saturable and involves an uptake rate constant (one for the spleen and another for all other organs), a single release rate constant and a single maximal uptake capacity constant. In models developed to describe the kinetics for uptake of nanoparticles *in vitro*, more process steps are included than in our model, *i.e.*, adherence to the cell membrane prior to engulfment and reprocessing of receptors required for endocytosis (Wilhelm *et al.*, 2002; Ohta *et al.*, 2012). We considered incorporation of *in vitro* models for phagocytosis into our own, but since extensive experimental data is not available this could lead to over-parameterization.

The modelling suggested that PAA-PEG had a preference for blood and a partition coefficient between tissue and blood was introduced to describe this behaviour. The partition coefficient may reflect the dynamic formation of corona formed around the nanoparticles, but the mechanism behind this is not fully understood. Corona formation is a dynamic process that is highly influenced by the properties of the nanoparticles, such as size, surface charge, shape and coatings and the biological environment (Cedervall *et al.*, 2007; Nel *et al.*, 2009).

Another difference with our model compared with other models is the inclusion of a parameter to account for residual blood in organs after harvesting. The experimental data on PAA-PEG indicated that levels in blood and brain were correlated, with parallel curves. In addition, when analysed, the brain contained residual blood. Therefore, we assumed that the blood-brain barrier is impermeable and that nanoparticles are actually present in residual blood. If residual blood is not taken into consideration, the conclusion may be that the nanoparticles are taken up, even when they are not (Frigell *et al.*, 2014). Unfortunately, biodistribution studies rarely report how harvesting was carried out and the measured level of nanoparticles in organs as brain and heart is often low. This makes measurement, visualization and model optimization challenging and sometimes uncertain.

5.1.2 Expansion of the PBPK model to other nanoparticles given intravenously

To investigate how generalizable the model developed in Paper I was for other nanoparticles considered inert, the model was applied to three additional types of nanoparticles (Paper II). In total, data sets from four different types of nanoparticles were used: PEGylated polyacrylamide (PAA-PEG), polyacrylamide (PAA), gold and titanium dioxide (TiO_2).

The data sets for these four particle types differed substantially both in nanoparticle properties and study design. Despite this, the model adequately described the biokinetics for all four, excepting the slow decrease with time observed for the amounts of gold and titanium dioxide in organs with low content, such as heart (R^2 on the log scale ranging from 0.88 to 0.96).

The differences in properties among the four types of nanoparticles were reflected by differences in values of nanoparticle-dependent model parameters. PAA and PAA-PEG had more similar values than gold and titanium dioxide. PAA was more readily cleared from blood than PAA-PEG, as a result of a 3-fold higher uptake rate constant to phagocytic cells. On the other hand, clearance from blood was much faster for gold and titanium dioxide than for PAA and PAA-PEG. According to the model, this was partly a result of faster uptake into phagocytic cells in spleen (> 9-fold higher k_{sab0}) and easier access to liver, spleen, bone marrow and brain (> 100-fold higher X_{fast}) for gold and titanium dioxide, respectively, compared with PAA and PAA-PEG. The time courses for gold and titanium dioxide look similar but in fact also differ, mainly because the uptake rate by phagocytic cells was much higher for titanium dioxide than for gold (> 6-fold difference), and titanium dioxide had a higher preference for tissue than gold (P was 0.97 for titanium dioxide and 0.13 for gold), but lower permeability into tissues (5- to 9-fold).

Another interesting result was the dose dependence. Higher doses saturate the phagocytic cells, which profoundly modifies biokinetics. The doses used for PAA and PAA-PEG were more than 30 times higher than for gold and titanium dioxide. As a result of this, more phagocytic cells became saturated for PAA and PAA-PEG than for gold and titanium dioxide.

We tested different grouping of organs connected to the three permeability coefficients in the model. The results demonstrated that the best fitting was achieved when the high permeability coefficient (X_{fast}) was assigned to liver, spleen and bone marrow. This grouping also reflected the anatomical structure of endothelium most accurately (Sarin, 2010; Setyawati *et al.*, 2015). In addition, and in contrast to Paper I, a low permeability over the blood-brain barrier had to be implemented to describe the levels of gold and titanium dioxide in brain.

The results from the sensitivity analysis demonstrated that even if the model structure is the same for all four types of nanoparticles, the different values on model parameters resulted in totally different sensitivity coefficients. In this study, this is partly a consequence of the saturation level of phagocytic cells. Our results suggest that sensitivity analysis cannot be done only once; it should preferably be updated when model parameters are changed.

5.1.2.1 Data for modelling

PBPK modelling requires data. To collect data for Paper II, we carried out an extensive literature review. However, as we and other researchers have experienced, access to published data useful for modelling is sparse. Partly, this is a result of study objectives differing from ours. In all biodistribution studies reviewed, the majority of reported aims focused on comparing biodistribution profiles for different nanoparticles, identifying target organs, or linking toxicity to a target dose.

For our purposes (Paper II), we reviewed data reported for nanoparticles with a variety of properties and applications, including gold, silver, titanium dioxide, silica and polymers, administered to rats via a single intravenous injection. These data exhibited serious limitations for modelling, including: (1) incomplete characterization of the nanoparticles and dose, (2) short follow-up after dosing, (3) analysis of only a few samples per tissue and only a few tissues per organ, (4) failure to account for the mass balance, and (5) lack of confirmation of nanoparticle integrity in the tissues. Such limitations make modelling of the time course, half-life and bioaccumulation difficult. Overall, our review revealed the complexity involved in drawing general conclusions about nanoparticle biodistribution, with no individual factor such as size, coating, shape, charge, chemical composition or agglomerations providing a complete explanation. In choosing among all reviewed studies (> 200 data sets), we decided to focus on inert nanoparticles and three additional data sets were found.

In short, the quality of the data sets used has a large impact on the modelling result and therefore we recommended in Paper II that new biodistribution studies should preferably involve*: "1) extensive characterization of NPs (size, size distribution, integrity, etc.), 2) monitoring of several organs at several time points, 3) frequent sampling immediately after dosing, 4) long follow-ups, 5) determination of the mass balance (total recovery), and 6) a detailed description of the analytical procedures employed (specificity, limits of detection, background levels, etc.)".*

5.1.2.2 Model structure and parameters

The description of uptake capacity of phagocytic cells was modified by separating the phagocytic uptake capacity constant in Paper I into two constants. The first constant reflected the uptake capacity of an individual phagocytic cell (nanoparticle-dependent) and the second constant described the density of phagocytic cells in the tissue (nanoparticle-independent). This separation makes it possible to compare uptake capacity of phagocytic cells predicted by the model with experimental data from *in vitro* studies.

The predicted uptake capacity of an individual phagocytic cell for the particles of PAA-PEG, PAA, gold and TiO_2 are in the range of those previously reported *in vitro* (Alkilany *et al.*, 2010; Ferrari *et al.*, 2014). The model suggested that the maximum uptake capacity is in the range of 0.5-5 pg per phagocytic cell, which corresponds to 2,000-300,000 NPs per phagocytic cell. Alkilany measured an uptake of 45-150,000 gold nanoparticles per cell and Ferrari and co-workers reported 45-10,000,000 polymeric nanoparticles per cell, depending on cell line, composition, size, charge and dose of nanoparticles. Hence, the *in vitro* values varied substantially, by several orders of magnitude. These large differences in uptake rate may reflect differences in nanoparticle properties, but also the method used to measure and model the uptake. In fact, the cellular dose in an *in vitro* system depends on how the nanoparticles interact, diffuse, settle and agglomerate in the cell medium (Teeguarden *et al.*, 2007; Hinderliter *et al.*, 2010; Cohen *et al.*, 2013).

The finding that the prediction of brain levels of PAA on the basis of residual blood is not as accurate as for PAA-PEG may reflect a slight difference in the way the organ was harvested, leaving a smaller amount of blood for PAA than for PAA-PEG. However, residual blood cannot explain the biokinetics of gold and TiO_2 nanoparticles with respect to the brain, since the level in blood approaches background levels. In these cases, brain levels must represent something else, probably uptake, in line with what has been observed by other researchers (Sonavane *et al.*, 2008; Kolhar *et al.*, 2013; Yokel *et al.*, 2013a; Frigell *et al.*, 2014; Geraets

et al., 2014). These problems with residual blood illustrate the importance of an accurate description of how organs are harvested, which, unfortunately, is often lacking and contributes uncertainty in the modelling results.

5.1.3 Expansion of the PBPK model to nanoceria administered by various routes

As a next step, we wanted to model the systemic distribution of cerium dioxide nanoparticles (nanoceria). We first collected experimental biodistribution data on nanoceria in rats (various exposure routes, sizes, coatings and tissues sampled) from the literature. Next, the PBPK model was calibrated and validated against data for 30 nm citrate-coated nanoceria, followed by recalibration and revalidation for 5 nm nanoceria. Finally, the model was modified and tested against inhalation, instillation and oral nanoceria data.

The model adequately described ($R^2 = 0.91$) and predicted the biokinetics of 5 nm nanoceria infused into rats, but failed to do so for other sizes, although some predictions were reasonable, *e.g.*, for liver and spleen. The 5 nm model could predict the values of new data within 2-fold for 17 out of 24 values for the 5 nm nanoceria, but the model under-predicted the concentration in blood at every time point for 3 nm nanoceria with a coating different from that of the 5 nm data sets. On the other hand, this result is in agreement with the opinion of Heckman and co-workers (Heckman *et al.*, 2013).

The experimental studies collected for 5 nm nanoceria were more similar than the studies for 30 nm nanoceria, both as regards the properties of the nanoparticles used and the study designs. This probably explains our problem in describing the biokinetics for the 30 nm nanoceria. The doses administered for 30 nm nanoceria ranged between 6 and 750 mg/kg, whereas the doses ranged between 10 and 85 mg/kg for 5 nm nanoceria. The experimental data for the 30 nm nanoceria suggested dose-dependent biokinetics. When the concentration was increased from 6 to 87 mg/kg, the concentration-time profile in blood, kidney and lung changed over time and 3 months after the administration of the highest dose the concentration increased. This behaviour cannot be described by the existing model and the mechanism behind it is not fully understood. However, a higher dose may trigger an inflammatory response resulting in recruitment of phagocytic cells. Phagocytic cells may dissolve the nanoceria and thereby change the biokinetics. Dissolution of nanoceria has been observed and cerium ions have been demonstrated to have a different biokinetic profile than nanoceria (Graham *et al.*, 2014; Molina *et al.*, 2014). On the other hand, the biodistribution profile for ions cannot explain the change in biokinetics for 30 nm nanoceria, which suggests a more complex mechanism.

In agreement with the conclusions of previous researchers, the compilation of data from biodistribution studies on inhalation, instillation and oral exposure points to a low systemic uptake. Less than 1 mass % (median) of the lung burden was transported to the liver and less than 0.01 mass % (median) of the administered oral dose was distributed to the liver, Figure 4.

Plotting the concentration ratios between organs (blood:liver, spleen:liver, brain:liver) over time suggested substantial dependence on the administration route (iv, inhalation, instillation, and ingestion). The ratios differed by several orders of magnitude and the shape of ratio-time curves varied. In comparison, the ratio-time curve following intravenous administration differed marginally between studies, in spite of the different sizes, coatings and doses,

whereas studies using other exposure routes showed ratio differences several orders of magnitude greater.

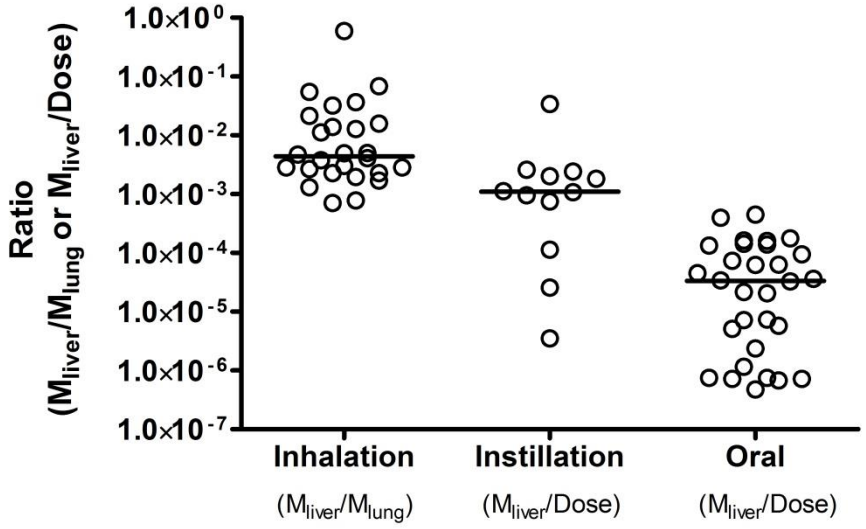

Figure 4.Comparison of experimental data on nanoceria by plotting the ratios between amount in liver and amount in lung or dose after inhalation, instillation and oral exposure in rats (Park et al., 2009; He et al., 2010; Nalabotu et al., 2011; Geraets et al., 2014; Keller et al., 2014; Kumari et al., 2014a; Kumari et al., 2014b; Molina et al., 2014; Konduru et al., 2015a; Li et al., 2016).The circles represent individual data and the solid line is the median value.

Re-optimization of the model to inhalation, instillation and oral exposure was not successful, mainly because the absorption via these routes was low, with low and variable nanoceria levels in tissues. Despite this, the time course pattern appeared to differ from the intravenous data and proved hard to reproduce.

Overall, our modelling results suggest that the biokinetics of nanoceria depend not only on the nanoparticle properties (size, coating), but also on the exposure conditions (dose, exposure route).

5.1.3.1 Model structure and parameters

The model structure was the same as in Paper II, but modified to include systemic uptake from the lung and gastrointestinal tract. The implemented modifications to the model were not successful and the modified model could not describe the systemic distribution of experimental data from inhalation, instillation and oral exposure. However, a complicating factor during modelling was access to rich data sets. Moreover, experimental data reported low uptake of nanoceria via these types of exposure routes, making the levels in internal organs low with large variability and often no significant differences between the organs.

Despite these limitations, the model structure may be too simplistic to describe the uptake process in the lung and gastrointestinal tract. In the lung, deposited nanoparticles can be transported via mucociliary clearance to the larynx followed by swallowing into the gastrointestinal tract (Oberdörster, 1988; Snipes, 1989). Mucociliary clearance is described in the model, but not translocation into the stomach and potential later systemic uptake from this

region. On the other hand, the uptake from the gastrointestinal tract appeared to be much lower than from the lung and the clearance rate from the lung is much lower than in the gastrointestinal tract, making exposure from the lung almost continuous.

In the lung, particles can also translocate into the lymphatic system, which the model does not describe. On the other hand, data in local lymph nodes were only reported in one of seven studies. In this model the lung is described with one compartment, which might be too simplistic. In Paper IV, we introduce a more complex structure for the lung.

The gastrointestinal tract is, like the lung, only represented as a single compartment. Here too, the systemic uptake may be more complex than a first-order absorption rate constant into the systemic circulation. Once again the lymphatic system is not included in the model, but none of the collected studies reported such data.

5.1.4 Further refinement of the PBPK model to account for inhalation exposure

The PBPK model was refined to account for the complexity of inhalation exposure using data generated within the study, from a short-term inhalation exposure to aged and pristine nanoceria in rats. The model includes mucociliary clearance, olfactory uptake, phagocytosis, and entry into the systemic circulation by alveolar wall penetration. The PBPK model described the biodistribution well and again suggested phagocytosis as a key process for biokinetics.

No significant differences either in biodistribution or properties between aged and unaged nanoceria were found. The majority of inhaled nanoparticles were recovered in the lung or in faeces and the levels decreased over time. Despite differences in the inhaled dose, the amount of nanoceria recovered in extrapulmonary organs was similar, within 65 % of each other. We think this reflects the amount of smaller particles with sizes less than 70 nm. According to the scanning mobility particle size data, this fraction of particles varied less than 31%. The majority of nanoceria was recovered in faeces, followed by the lung. In total, less than 4 % was detected in extrapulmonary organs.

The model, expanded to inhalation exposure, described the measured data in the four experiments well (R^2 on the log scale ranging from 0.68 to 0.95). However, the increase in levels in extrapulmonary organs could not be captured.

The model predictions were sensitive to changes in model parameters, such as the fraction of inhaled nanoparticles deposited in the upper airway and in the pulmonary region, the faeces clearance rate from the GI tract, the uptake rate from the GI tract, the partition between blood and tissue and the permeability coefficient connected to lung, kidney, heart and carcass.

5.1.4.1 Model structure and parameters

The model structure for the systemic distribution was the same as in Paper II, but expanded to include the respiratory system. To describe the respiratory system, a similar structure as that used by Sweeney and colleagues was added to the model (Sweeney *et al.*, 2015; Carlander *et al.*, 2016). The respiratory system was represented by three compartments: 1) the upper airway, 2) the tracheobronchial region, and 3) the pulmonary region and the gastrointestinal tract with one compartment.

Following inhalation, nanoceria are deposited in the three regions. Deposited nanoparticles can be cleared (Oberdörster, 1988). In the upper airway, the model assumes that swallowing into the gastrointestinal tract clears the nanoceria. In the tracheobronchial region, the main clearance mechanism is the mucociliary escalator to the larynx and further transport into the gastrointestinal tract (Oberdörster, 1988; Snipes, 1989). In the pulmonary region, the particles can be engulfed by alveolar macrophages and transferred to the bronchial region or translocate into the interstitium.

Initially, we tried to use the deposition fraction calculated from the Multiple-Path Particle Dosimetry Model (MPPD v 2.11), but this was not successful. The strategy was changed and the deposition was fitted to observed data instead, assuming the same deposition fraction for all four runs. Interestingly, the fitted deposition fractions in the tracheobronchial and pulmonary regions calculated using the expanded PBPK model were lower than those calculated using the Multiple-Path Particle Dosimetry Model (MPPD v 2.11), while the deposition fraction in the upper airway region was higher. This could be explained by agglomeration. The original size of the nanoceria is 2-3 nm, but on their way to the animals the nanoceria agglomerate, as recorded by the scanning mobility particle sizer (SMPS) measurements. It is likely that the agglomeration continues after the SMPS measurements until the nanoceria get inside the animals, as the equipment is not in direct contact with the animals. Moreover, in the respiratory system the air conditions change and become more humid, which may increase agglomeration. Increased agglomeration leads to a higher deposition fraction in the upper airways, with fewer particles reaching the lower respiratory regions.

More than half of the recovered amount of nanoceria was found in faeces. This was much higher than the fraction reported by He and colleagues, who had approximately 20 % dose recovery in faeces (He *et al.*, 2010). On the other hand, He and co-workers used instillation with a bolus dose, which excludes deposition outside the lung, limiting transport to the gastrointestinal tract only to mucociliary clearance. In this study, the nanoceria were delivered in a nose-only inhalation chamber and deposition in the upper airway, as well on the whiskers and snout, will take place and contribute to the ingestion of nanoceria. In whole body exposure chambers, deposition on the fur followed by licking also adds to the ingestion of nanoceria. Unfortunately, many studies do not report the amount in faeces, urine and total recovery, which limits the ability to compare results and develop nano PBPK models. For nanoceria, the model predicted that the uptake to extrapulmonary organs mainly came from translocation from the lung. This is in agreement with other researchers, who have reported that uptake from the gastrointestinal tract is lower than from the lung (Yokel *et al.*, 2012; Molina *et al.*, 2014).

Several research groups have showed that, in the lung, nanoparticles translocate to the lymphatic system, that this translocation depends on nanoparticle properties, such as size, and that it increases with increased lung burden (Tran *et al.*, 2000; Choi *et al.*, 2010; Keller *et al.*, 2014). Our model does not include the lymphatic system, mainly because we did not have access to such data. Adding a compartment for the lymphatic system without the ability to calibrate this to experimental data would increase uncertainty and enhance the complexity of the model. We therefore decided to exclude the lymphatic system until data was available. In our study, the lymph nodes around the lung were not removed before the lung was analysed. Even if the concentration in the local lymph nodes would be high, the amount in local lymph nodes would contribute negligibly to the overall amount in the lung, because of their small

size and limited translocation. In our study, the inhalation concentration was more than ten times lower compared with studies showing increased translocation to the lymph nodes (Keller *et al.*, 2014). In other studies, we have noticed that it is often unclear whether lymph nodes have been removed or not before analysis of the lung.

Another limitation with this study is the large variability in some of the experimental data, which may result from for example the individual behaviours of rats, differences in delivered concentration and methodology. This variability combined with low concentration in extrapulmonary tissues contributed to uncertainties in the optimization of the model.

5.2 DISSOLUTION OF GOLD NANOPARTICLES

Most published PBPK models for nanoparticles, including our own, do not include dissolution processes of nanoparticles. One explanation might be that the common opinion is that nanoparticles used for modelling, such as gold, titanium dioxide, nanoceria and quantum dots, do not dissolve during the relatively short time period described by models. However, if models are going to be used for humans, long-term exposure scenarios are required and then dissolution of nanoparticles might be a relevant, even critical, process (Misra *et al.*, 2012; Utembe *et al.*, 2015; Feliu *et al.*, 2016a). Another aspect is that the biokinetics and the toxicities of dissolved entities may differ from those of the particles (Molina *et al.*, 2014; Sabella *et al.*, 2014). Consequently, if dissolution takes place, this process should be implemented into PBPK models. Implementing dissolution processes into a PBPK model might seem straightforward, but in fact it is not, because the models get more complex and require experimental data on the biokinetics of nanoparticles and dissolution species that are not yet available. In addition, the kinetics of dissolution of nanoparticles considered inert, such as gold in a biological environment, have not yet been described in the literature.

In Paper V, we wanted to challenge a common opinion that gold is inert. This was due to results from our modelling efforts in Paper II suggesting that gold might dissolve over time. Combined with information from the literature, this triggered us to create a hypothesis: Gold can be dissolved by macrophages.

To test this hypothesis, an *in vitro* method was developed to compare the dissolution of AuNPs in i) cell medium, ii) macrophages, and iii) LPS-triggered macrophages (simulating inflammatory conditions), using Inductively Coupled Plasma Mass Spectrometry (ICP-MS) measurements of gold in the media.

We exposed the *in vitro* system to 5 µg/ml of 5 nm and 50 nm gold nanoparticles for 0, 24 and 168 h (1 week). A clear, time-dependent dissolution of the 5 nm AuNPs was seen already in the cell medium, corresponding to 3 % and 0.6 % of the added amount of 5 nm and 50 nm AuNPs, respectively, after 1 w (168 h) of incubation. The dissolution of 5 nm AuNPs was further increased to 4 % in the presence of macrophages and reached 14 % after LPS-triggering. In contrast, no such increases were observed for 50 nm AuNPs, except after 1 w in the presence of LPS.

The size-dependent dissolution of gold nanoparticles in cell medium (without cells) can be explained by differences in surface area and agglomeration. We observed lower differences (three- to six-fold) in dissolution than would be expected from surface area differences (ten-fold), but on the other hand, 5 nm nanoceria appear to agglomerate more than 50 nm nanoceria, which would reduce the differences. In contrast, dissolution in the presence of

triggered macrophages cannot be explained by increased agglomeration or uptake of 5 nm nanoceria. In agreement with results reported by other researchers, we found higher cell doses (NPs taken up or attached to cells) for the 50 nm AuNPs (approx. 80 % of added amount) than for the 5 nm (approx. 60 %) after 24 h (Chithrani *et al.*, 2006). After 1 week, the dissolution was 5-fold higher when 5 nm nanoceria were exposed to triggered macrophages than when exposed to the cell medium only, whereas for 50 nm nanoceria, the dissolution was only slightly increased. A more likely explanation is that the inherent properties of the small AuNPs, such as higher surface energy, catalytic activity and defects of the surface, are the main reasons for the observed difference in gold dissolution in the presence of macrophages (Clarke *et al.*, 2001; Zhou *et al.*, 2010).

We were interested in the total release of dissolution products from gold, *i.e.*, both inside, on, and outside the cell, and therefore both the cell medium and the cells were collected at the end of incubation. The cells were mechanically sheared to provide a cell lysate before being mixed with the cell medium. In practice, the separation of small gold nanoparticles and dissolved gold ions/complexes turned out to be an experimental challenge, especially for our gold nanoparticles incubated in cell medium (only). When we added unexposed cell lysates to the gold nanoparticles incubated in cell medium (only), the centrifugation efficiency was improved and the variations in results reduced. This novel but simple process ensured similar test conditions for all samples.

When macrophages are triggered with LPS, a condition of oxidative stress is induced and the production of reactive oxygen species is elevated (Forman *et al.*, 2002; Gantner *et al.*, 2003). Hydroxyl radicals are reactive oxygen species with high redox potential, even higher than gold, and consequently dissolution of gold through an electrochemical process is possible (Mohr, 2009). We therefore expected that triggered macrophages would increase dissolution, which was confirmed in this study.

The high redox potential of gold suggests that gold is not easily dissolved and released gold ions will easily be reduced back to elementary gold. To test if the method could detect gold ions in the cell medium, we performed a recovery test by incubating cell medium with gold ions followed by lysate-assisted centrifugation. We added gold ions (0.25 µg in 1 ml) to the cell medium, and recovered approximately 70 % of the added gold amount. As expected, a lower percentage was detected when higher concentrations were used (1 and 5 µg in 1 ml). This is interesting because it is far higher than the results from classical thermodynamic equilibrium modelling (Joint Expert Speciation System, version 8.3). According to the modelling, only 0.4 % (for the highest gold concentration of 5 µg/mL) and 8 % (for the lowest gold concentration of 0.25 µg/mL) would be in solution as gold hydroxide (AuOH). However, thermodynamic equilibrium modelling only includes certain components in cell medium as input for calculations of properties in test medium, such as pH and ion strength, but possible reactions between gold and biological substances in the medium is not accounted for. Indeed, our results suggest that such reactions are critical and gold has been shown to interact with thiols, cyanides and amino acids (components of cell medium and lysed cells), generating ligands with dissolved gold ions (Brown *et al.*, 1982; Larsen *et al.*, 2007; Mohr, 2009; Paulsson *et al.*, 2009). The next step is to identify where the dissolution takes place, characterize the constitution of the gold ions/complexes formed and take a closer look at the dynamics and processes inside the cells. Another improvement would be to update classical thermodynamic equilibrium models with information about reactions between gold and biological substances.

6 CONCLUSIONS

In this thesis, a PBPK model for nanoparticles considered inert has been developed. The model adequately describes the biokinetics of different types of inert nanoparticles given intravenously into rats, despite large differences in properties and exposure conditions (PAA-PEG, PAA, gold, titanium dioxide and nanoceria). In addition, after modification to account for the complexity of inhalation exposure of nanoparticles, the model well captured the biokinetics of nanoceria inhaled by rats. Uptake of nanoparticles by phagocytic cells was identified as a critical process. This process is saturable and has great impact on the biokinetics of nanoparticles. Our model was the first to include saturable phagocytic cells and has been copied by other research groups and we argue that phagocytic cells should be a natural compartment in nano PBPK models. However, nano PBPK models are still in their infancy and require further development to better reflect processes such as agglomeration, corona formation and dissolution.

Validated PBPK models can describe and predict how substances are taken up, distributed, degraded and excreted from the body, even when the relationship between external and target dose is non-linear. Our results indicate that this is the case for biokinetics of nanoparticles, meaning that a validated nano PBPK model would be of great value to risk assessors, who often need to extrapolate exposure risks for humans on the basis of animal data. Our model represents a first step in that direction. In the future, it needs to be validated for different exposure routes and species. This was not yet possible, because experimental data are not available. In a next step, more experimental data are needed to predict the behaviour of new types of nanoparticles in order to link their properties to model parameters.

PBPK models are not limited to use only in risk assessment. This thesis clearly demonstrates that modelling also contributes to evaluating the quality of biodistribution studies, identifying knowledge gaps, and to generation and testing of hypotheses.

The review of biodistribution studies points to the need for improved control and reporting of study results. Such improvements should involve more detailed reporting of nanoparticle characteristics and methodology.

Even though a lot has been published on how the biokinetics of nanoparticles are influenced by their properties (such as size, shape, surface chemistry, and agglomeration) and their interaction with the bio-environment (corona formation, phagocytosis, dissolution), these factors are not well characterized in quantitative terms and thus not readily implemented in PBPK models for nanoparticles. This illustrates the need for quantification of such factors.

The modelling efforts also demonstrate that results may lead to new hypotheses, as in Paper II, where we generated a hypothesis that gold is dissolved by macrophages. In Paper V, we tested the hypothesis and demonstrated that macrophages *in vitro* can dissolve gold nanoparticles.

7 FUTURE PERSPECTIVES

The existing nano PBPK models are of limited use for risk assessment, since they cannot readily be applied to new types of nanoparticles, species or conditions of exposure without access to experimental data. Improvement of available models requires appropriately designed investigations of biodistribution. Today, for example, most published PBPK models are limited to short-term exposure and single doses. To make models useful for humans, long-term exposure and repeated doses need to be implemented. Extrapolating short-term results to long-term and repeated exposure is not recommended because the rate-limiting factors driving the biokinetics may change over time. So far data for such exposure conditions are sparse; thus, this field needs further attention.

Another important improvement of study designs would be to combine *in silico*, *in vitro* and *in vivo* approaches, which would help to answer some of the currently most urgent questions in the field: Can we choose model parameters on the basis of the physicochemical properties of the nanoparticles? What key factors, including species differences, dictate the biokinetic behaviours of these particles? How do we implement the dynamic behaviour of corona formation, agglomeration and dissolution into our models?

In addition to extrapolating and combining current findings/knowledge to predict the impact of nanomaterials on different organs and different species, *in silico* procedures, such as principle component analysis (PCA), quantitative structural activity relationship (QSAR/QNAR) and PBPK, can help in the design of robust *in vivo* studies by providing information about, *e.g.*, structural patterns in data, relationships between parameters and toxic endpoints, and appropriate dosing and sampling frequencies.

Continuous improvements of *in vitro* methods make them more and more similar to the *in vivo* situation. Today, we know much about the mechanisms by which nanoparticles are taken up by cells, but less about uptake kinetics and even less about nanoparticle release.

Most important for good PBPK model development is access to experimental data. However, data on physiological parameters are unfortunately not as easily found as we thought. Databases developed for collection of such data are often not public and those that are public are often not updated. Requiring the reporting of such data into databases, as carried out for reporting of genomes, would improve the quality of models, as well as contributing to the 3Rs (reduction, refinement and replacement) of animal testing.

My belief is that focus and cross-scientific collaboration will generate useful nano PBPK models in the future. But, as usual, hard work is required.

8 ACKNOWLEDGEMENTS

Thanks a lot to the financial supporters of my research project.

- The Swedish Research Council for health Working Life and Welfare (Forte, grant No 2010-0702), Sweden,
- The NANoREG project of the European Union Seventh Framework Programme (grant No 310584), and
- IMM´s funding of strategic grants for pilot collaboration projects, Karolinska Insitutet, Sweden.

Gunnar Johanson. It has been a true honour to have you as my supervisor. You have immensely supported my understanding of the scientific world. This has been truly valuable. I do however have to admit that there have been periods where my frustration level has reach new levels. Your inputs on my writing have been exceptional. Before I got used, I read the first drafts with mixed emotions, now I really look forward to reading them as I learn so much. You have a fantastic sense for structure. You combine this ability with a tremendous eye for details, and a knowledge base that is exceptionally broad. On top of that you are caring when the need occurs. It has been a true honour.

Hanna Karlsson, you are fantastic. The level of energy you bring to a meeting makes one wonder why we need nuclear plants at all. Your way of being is in itself a reduction of the human environmental footprint. It has been inspiring to have you as a co-supervisor. When we at last, after all conversations, got the opportunity to design and perform a study together, we had so much fun. Despite its simplicity, it became a golden story that I will remember with a lot of joy. You are super.

Lennart Lindbom. Never in my life I would have understood that the structure and function of endothelium (blood vessels for the normal population) could be as complex as it in truth is. On the other hand, maybe I should have realized, just by the name glycocalyx (the name of the hairs that grow on the inner walls of blood vessels)…. It has been a pleasure to tap your brain on a fragment of your overwhelming expertise and dig into your field of research, fascinatingly interesting and fundamentally complex. You are one of a kind.

Lars Magnus Bjursten, the very best mentor ever!!! I have learnt so much from you. I like your style. You are brave, a bit eccentric but above all supportive. There is never a situation that hinders you from giving inspiring and at the same time (oddly enough) constructive support. It is to no-bodies surprise that you have succeeded to such levels. A million thanks for all your support. You are fantastic.

Dingsheng Li. It has been a pleasure to work with you. Your stubborn, inspiring, gentle, polite push when you are convinced that you know the answer has challenged my intellect and made me think in new ways. I think we have learnt a lot from each other on our way to become independent researchers. In any case I know that I have learnt a lot from you. I have appreciated your comments and our discussions. Thanks and good luck with your future ventures. I hope our future cooperation will take us both far.

Claude Emonde and Olivier Jolliet, many thanks for your support in the field of developing PBPK models for nanoparticles. It has been a pleasure to ventilate problems and solutions on

improvement of the models. You have truly enriched my research and made it more competitive.

I also want to acknowledge my co-authors in Paper I, Martin Philbert and in Paper IV, Masako Morishita, James G Wagner, Mohammad Fatouraie, Margaret Wooldridge, W. Ethan Eagle, James Barres. Thanks for letting me be a part of your research.

Klara Midander. You are my joyful, funny whirlwind and inspiring colleague. Our conversations have made me understand that I actually bring something to the research environment in which I try to contribute. Your belief in people releases their ability to perform.

Yolanda Hedberg and Matteo Bottai. Thanks for sharing your expertise in materials characterisation and statistical analysis respectively during our collaborations. Without your contributions, no Paper V would ever reach outside the corridor of the IMM building.

Robert Yokel, the gentleman from the other side of the pond, who kindly volunteered all his valuable data to us. Thank you for the opportunity to work with you. Your encouraging support has brought the PBPK modelling forward.

Robin MacDougel, Marc Andre and Conrad Houser, thanks for all your support. You have patiently handled my impatiens in learning acslX Libero, and now when I can handle it reasonably independently, acslX is no longer available on the market. Luckily it still runs on my computer.

Audrey Gallud, Sebastiano Di Bucchianico, Francesca Cappellini, Anda Gliga, Siiri Latvala, and Behnaz Erfani for all the support in the lab. You all contributed to my Paper V.

Emma Vincent, Stephanie Juran and Mia Johansson, thanks for taking me out of the office for exercises, "chat walks", chocolate production, reflections on life and the world as a whole, the importance of things and more. With colleagues like you, life is just so much easier. The magnitude of things gets so much more reachable. It has been so very appreciated and relaxing.

Aishwarya Mishra, Anna-Karin Mörk, Carolina Vogs, Elin Törnqvist, Joakim Ringblom, Johanna Bengtsson, Kristin Larsson, Kristin Stamyr, Linda Bergander, Linda Schenk, Martin Fransson, Tao Liu, Matias Rauma, and so many more. In Swedish society the ability to have a valuable lunch chat is of essence. You have substantially contributed in making this every day experience.

The colleagues at Unit of Work Environmental Toxicology, Arbetsmiljöverket, Gentekniknämnden, and lately also Occupational and Environmental Dermatology, and Lung and Airway Research, you have contributed through enriching the important Swedish fika-conversations. You contribute to the coffee consumption in Sweden and to foreigners feeling the power of integration into the Swedish working society. I'm glad that I have had the opportunity to be a part of such a nice workplace.

Annika Hanberg, Johanna Zilliacus, Charlotte Nilsson, Ralf Morgenstern, Kristian Dreij and Emma Vincent, thanks for letting me be part of the team educating of the master students in toxicology and biomedicine. It has been so enjoyable and inspiring. You are a perfect mega super team.

Doctoral education board, I humbly thank you for supporting my development as an independent researcher. You have given me insight into the process of qualifying projects as well as candidates for successful research projects.

All ambitious students of the toxicology and the biomedical programs. You have supported my educational skills. It has been a joy and I wish all of you a prosperous future.

A specially thanks to Anteneh Assefa Desalegn, who allowed me to be his supervisor during his master project and to Tshepo Moto, who continue the nanoceria modelling work after Anteneh.

Not to forget, I would like to give my greatest gratitude to all collaborators and knowledgeable people around the world that I have met during my doctoral education. You contributed greatly to my education and made it such an instructive and memorable period.

Familjen. Ni är bäst!!! Tack för att ni finns, ställer upp, tar ansvar och sköter er så bra. Nu är det över och vi får förhoppningsvis mer tid tillsammans. Nu blir det tid för annat som jag vet att ni mina underbara och fantastiska barn ser fram emot. Men lugn min SUPER-John, vi ska ta det lugnt också, prata och diskutera och kanske göra något som du gillar som att spela golf och fixa så vi får bättre ordning i hemmet. Tack också John för alla långa stunder av diskussioner om matematiska metoder och statistisk relevans och för att du som en svamp sugit upp min frustration när den varit på topp.

Jag saknar er mycket Mamma och Pappa. Ni fick tyvärr aldrig vara med om detta, men jag vet att ni skulle ha varit jättestolta. Tyvärr Pappa, gick du bort precis innan jag hann bli klar. Jag är dock tacksam för att du fick vara med ett tag. Det betydde mycket.

Tack syrran för ditt stöd. Det har hänt mycket de senaste åren. Det känns bra att ha en syster som man kan prata med och besöka lite då och då. Familjen, släkten och vännerna i Sundsvall, ni betyder mycket för oss i Solna.

Vibeke, vad skulle jag göra utan dig. Ditt stöd är fantastiskt. Du hjälper till med allt, från att städa, laga mat, läsa läxor med barnen till att granska mina dokument och diskutera intressanta ämnen och utforska världen. Vad mer kan man begära av en svärmor, möjligtvis att vi bodde närmare varandra. Du är en klippa.

A big hug to all my friends, to all of you who have made my spare time rich and fun. What would life be without you? Less worth living. You are fantastic.

Finally, I would like to express a special gratitude to Linnea Holmén, Vibeke Carlander, John Carlander, Lars-Magnus Bjursten, Anneli Julander, Klara Midander, Joakim Ringblom, Linda Schenk, Stephanie Juran, Hanna Karlsson and Gunnar Johanson for your precious support during my kappa writing and for all the useful tips on the dissertation process I got from Joakim Ringblom, being just in from of me in this process.

9 REFERENCES

Aillon KL, Xie Y, El-Gendy N, Berkland CJ and Forrest ML (2009). "Effects of nanomaterial physicochemical properties on in vivo toxicity". *Advanced Drug Delivery Reviews* 61(6): 457-466.

Albanese A and Chan WCW (2011). "Effect of gold nanoparticle aggregation on cell uptake and toxicity". *ACS Nano* 5(7): 5478-5489.

Alkilany AM and Murphy CJ (2010). "Toxicity and cellular uptake of gold nanoparticles: What we have learned so far?". *Journal of nanoparticle research : an interdisciplinary forum for nanoscale science and technology* 12(7): 2313-2333.

Anjilvel S and Asgharian B (1995). "A multiple-path model of particle deposition in the rat lung". *Fundamental and Applied Toxicology* 28(1): 41-50.

Arts JHE, Hadi M, Irfan MA, Keene AM, Kreiling R, Lyon D, Maier M, Michel K, Petry T, Sauer UG, Warheit D, Wiench K, Wohlleben W and Landsiedel R (2015). "A decision-making framework for the grouping and testing of nanomaterials (df4nanogrouping)". *Regulatory Toxicology and Pharmacology* 71(2): S1-S27.

Bachler G, von Goetz N and Hungerbuhler K (2013). "A physiologically based pharmacokinetic model for ionic silver and silver nanoparticles". *International Journal of Nanomedicine* 8: 3365-3382.

Bachler G, Losert S, Umehara Y, von Goetz N, Rodriguez-Lorenzo L, Petri-Fink A, Rothen-Rutishauser B and Hungerbuehler K (2015a). "Translocation of gold nanoparticles across the lung epithelial tissue barrier: Combining in vitro and in silico methods to substitute in vivo experiments". *Particle and Fibre Toxicology* 12(1): 18.

Bachler G, von Goetz N and Hungerbuhler K (2015b). "Using physiologically based pharmacokinetic (pbpk) modeling for dietary risk assessment of titanium dioxide (tio2) nanoparticles". *Nanotoxicology* 9(3): 373-380.

Balashazy I, Hofmann W and Heistracher T (2003). "Local particle deposition patterns may play a key role in the development of lung cancer". *Journal of applied physiology* 94(5): 1719-1725.

Bazile D, Prud'homme C, Bassoullet MT, Marlard M, Spenlehauer G and Veillard M (1995). "Stealth me.Peg-pla nanoparticles avoid uptake by the mononuclear phagocytes system". *Journal of Pharmaceutical Sciences* 84(4): 493-498.

Bernareggi A and Rowland M (1991). "Physiologic modeling of cyclosporin kinetics in rat and man". *Journal of pharmacokinetics and biopharmaceutics* 19(1): 21-50.

Biozzi G, Benacerraf B and Halpern BN (1953). "Quantitative study of the granulopectic activity of the reticulo-endothelial system. Ii. A study of the kinetics of the r. E. S. In relation to the dose of carbon injected; relationship between the weight of the organs and their activity". *Br J Exp Pathol* 34(4): 441-457.

Borm P, Cassee FR and Oberdorster G (2015). "Lung particle overload: Old school -new insights?". *Particle and Fibre Toxicology* 12: 10.

Braakhuis HM, Cassee FR, Fokkens PHB, de la Fonteyne LJJ, Oomen AG, Krystek P, de Jong WH, van Loveren H and Park MVDZ (2016). "Identification of the appropriate dose metric for pulmonary inflammation of silver nanoparticles in an inhalation toxicity study". *Nanotoxicology* 10(1): 63-73.

Bradfield JW (1980). "A new look at reticuloendothelial blockade". *British Journal of Experimental Pathology* 61(6): 617-623.

Brain JD, Knudson DE, Sorokin SP and Davis MA (1976). "Pulmonary distribution of particles given by intratracheal instillation or by aerosol inhalation". *Environmental Research* 11(1): 13-33.

Briley-Saebo K, Bjornerud A, Grant D, Ahlstrom H, Berg T and Kindberg GM (2004). "Hepatic cellular distribution and degradation of iron oxide nanoparticles following single intravenous injection in rats: Implications for magnetic resonance imaging". *Cell and tissue research* 316(3): 315-323.

Brook RD (2008). "Cardiovascular effects of air pollution". *Clinical Science* 115(5-6): 175-187.

Brookes M (1967). "Blood flow rates in compact and cancellous bone and bone marrow". *Journal of Anatomy* 101: 533-&.

Brown DH, Smith WE, Fox P and Sturrock RD (1982). "The reactions of gold(0) with amino-acids and the significance of these reactions in the biochemistry of gold". *Inorganica Chimica Acta-Bioinorganic Chemistry* 67(1): 27-30.

Brown RP, Delp MD, Lindstedt SL, Rhomberg LR and Beliles RP (1997). "Physiological parameter values for physiologically based pharmacokinetic models". *Toxicology and Industrial Health* 13(4): 407-484.

Buzea C, Pacheco, II and Robbie K (2007). "Nanomaterials and nanoparticles: Sources and toxicity". *Biointerphases* 2(4): MR17-71.

Canton I and Battaglia G (2012). "Endocytosis at the nanoscale". *Chemical Society Reviews* 41(7): 2718-2739.

Cao Y, Li J, Liu F, Li XY, Jiang Q, Cheng SS and Gu YX (2016). "Consideration of interaction between nanoparticles and food components for the safety assessment of nanoparticles following oral exposure: A review". *Environmental Toxicology and Pharmacology* 46: 206-210.

Carlander U, Li D, Jolliet O, Emond C and Johanson G (2016). "Toward a general physiologically-based pharmacokinetic model for intravenously injected nanoparticles". *International Journal of Nanomedicine* 11: 625-640.

Cedervall T, Lynch I, Lindman S, Berggard T, Thulin E, Nilsson H, Dawson KA and Linse S (2007). "Understanding the nanoparticle-protein corona using methods to quantify exchange rates and affinities of proteins for nanoparticles". *Proceedings of the National Academy of Sciences of the United States of America* 104(7): 2050-2055.

Chen WY, Cheng YH, Hsieh NH, Wu BC, Chou WC, Ho CC, Chen JK, Liao CM and Lin P (2015). "Physiologically based pharmacokinetic modeling of zinc oxide nanoparticles and zinc nitrate in mice". *International Journal of Nanomedicine* 10: 6277-6292.

Chithrani BD, Ghazani AA and Chan WC (2006). "Determining the size and shape dependence of gold nanoparticle uptake into mammalian cells". *Nano Letters* 6(4): 662-668.

Choi HS, Liu W, Misra P, Tanaka E, Zimmer JP, Itty Ipe B, Bawendi MG and Frangioni JV (2007). "Renal clearance of quantum dots". *Nat Biotechnol* 25(10): 1165-1170.

Choi HS, Ashitate Y, Lee JH, Kim SH, Matsui A, Insin N, Bawendi MG, Semmler-Behnke M, Frangioni JV and Tsuda A (2010). "Rapid translocation of nanoparticles from the lung airspaces to the body". *Nature biotechnology* 28(12): 1300-1303.

Clarke NZ, Waters C, Johnson KA, Satherley J and Schiffrin DJ (2001). "Size-dependent solubility of thiol-derivatized gold nanoparticles in supercritical ethane". *Langmuir* 17(20): 6048-6050.

Cohen J, DeLoid G, Pyrgiotakis G and Demokritou P (2013). "Interactions of engineered nanomaterials in physiological media and implications for in vitro dosimetry". *Nanotoxicology* 7(4): 417-431.

Costa P, Manuel J and Lobo S (2001). "Modeling and comparison of dissolution profiles". *European Journal of Pharmaceutical Sciences* 13(2): 123-133.

Daigle CC, Chalupa DC, Gibb FR, Morrow PE, Oberdorster G, Utell MJ and Frampton MW (2003). "Ultrafine particle deposition in humans during rest and exercise". *Inhalation Toxicology* 15(6): 539-552.

Dan M, Wu P, Grulke EA, Graham UM, Unrine JM and Yokel RA (2012). "Ceria-engineered nanomaterial distribution in, and clearance from, blood: Size matters". *Nanomedicine* 7(1): 95-110.

Daniel MC and Astruc D (2004). "Gold nanoparticles: Assembly, supramolecular chemistry, quantum-size-related properties, and applications toward biology, catalysis, and nanotechnology". *Chemical reviews* 104(1): 293-346.

DeLorenzo AJD (1970). "The olfactory neuron and the blood-brain

barrier". *Taste and smell in vertebrates*. GEW Wolstenholme and J Knight. London, J&A Churchill**:** 151–176.

Demoy M, Andreux JP, Weingarten C, Gouritin B, Guilloux V and Couvreur P (1999). "Spleen capture of nanoparticles: Influence of animal species and surface characteristics". *Pharmaceutical Research* 16(1): 37-41.

des Rieux A, Fievez V, Garinot M, Schneider YJ and Preat V (2006). "Nanoparticles as potential oral delivery systems of proteins and vaccines: A mechanistic approach". *Journal of Controlled Release* 116(1): 1-27.

Di Silvio D, Rigby N, Bajka B, Mackie A and Bombelli FB (2016). "Effect of protein corona magnetite nanoparticles derived from bread in vitro digestion on caco-2 cells morphology and uptake". *International Journal of Biochemistry & Cell Biology* 75: 212-222.

Docter D, Westmeier D, Markiewicz M, Stolte S, Knauer SK and Stauber RH (2015). "The nanoparticle biomolecule corona: Lessons learned - challenge accepted?". *Chemical Society Reviews* 44(17): 6094-6121.

Donaldson K and Seaton A (2012). "A short history of the toxicology of inhaled particles". *Particle and Fibre Toxicology* 9: 13.

Dorier M, Brun E, Veronesi G, Barreau F, Pernet-Gallay K, Desvergne C, Rabilloud T, Carapito C, Herlin-Boime N and Carriere M (2015). "Impact of anatase and rutile titanium dioxide nanoparticles on uptake carriers and efflux pumps in caco-2 gut epithelial cells". *Nanoscale* 7(16): 7352-7360.

Duncan TV (2011). "Applications of nanotechnology in food packaging and food safety: Barrier materials, antimicrobials and sensors". *Journal of Colloid and Interface Science* 363(1): 1-24.

Elder A, Gelein R, Silva V, Feikert T, Opanashuk L, Carter J, Potter R, Maynard A, Ito Y, Finkelstein J and Oberdorster G (2006). "Translocation of inhaled ultrafine manganese oxide particles to the central nervous system". *Environmental Health Perspectives* 114(8): 1172-1178.

Elgrabli D, Beaudouin R, Jbilou N, Floriani M, Pery A, Rogerieux F and Lacroix G (2015). "Biodistribution and clearance of tio2 nanoparticles in rats after intravenous injection". *PLoS One* 10(4): e0124490.

Etheridge ML, Campbell SA, Erdman AG, Haynes CL, Wolf SM and McCullough J (2013). "The big picture on nanomedicine: The state of investigational and approved nanomedicine products". *Nanomedicine* 9(1): 1-14.

EU NanoSafety Cluster. (2016). from http://www.nanosafetycluster.eu/.

European Commission (2011). "Commission recommendation of 18 october 2011 on the definition of nanomaterials (2011/696/eu)". *Official Journal of the European Union*(L 275): 38-40.

Fadeel B, Fornara A, Toprak MS and Bhattacharya K (2015). "Keeping it real: The importance of material characterization in nanotoxicology". *Biochemical and Biophysical Research Communications* 468(3): 498-503.

FDA (2014) "Guidance for industry considering whether an fda - regulated product involves the application of nanotechnology".

Feliu N, Docter D, Heine M, del Pino P, Ashraf S, Kolosnjaj-Tabi J, Macchiarini P, Nielsen P, Alloyeau D, Gazeau F, Stauber RH and Parak WJ (2016a). "In vivo degeneration and the fate of inorganic nanoparticles". *Chemical Society Reviews* 45(9): 2440-2457.

Feliu N, Huhn J, Zyuzin MV, Ashraf S, Valdeperez D, Masood A, Said AH, Escudero A, Pelaz B, Gonzalez E, Duarte MAC, Roy S, Chakraborty I, Lim ML, Sjoqvist S, Jungebluth P and Parak WJ (2016b). "Quantitative uptake of colloidal particles by cell cultures". *Science of the Total Environment* 568: 819-828.

Ferrari R, Lupi M, Colombo C, Morbidelli M, D'Incalci M and Moscatelli D (2014). "Investigation of size, surface charge, pegylation degree and concentration on the cellular uptake of polymer nanoparticles". *Colloids and surfaces. B, Biointerfaces* 123: 639-647.

Filon FL, Crosera M, Adami G, Bovenzi M, Rossi F and Maina G (2011). "Human skin penetration of gold nanoparticles through intact and damaged skin". *Nanotoxicology* 5(4): 493-501.

Filon FL, Mauro M, Adami G, Bovenzi M and Crosera M (2015). "Nanoparticles skin absorption: New aspects for a safety profile evaluation". *Regulatory Toxicology and Pharmacology* 72(2): 310-322.

Forman HJ and Torres M (2002). "Reactive oxygen species and cell signaling - respiratory burst in macrophage signaling". *American Journal of Respiratory and Critical Care Medicine* 166(12): S4-S8.

Frey NA, Peng S, Cheng K and Sun SH (2009). "Magnetic nanoparticles: Synthesis, functionalization, and applications in bioimaging and magnetic energy storage". *Chemical Society Reviews* 38(9): 2532-2542.

Frigell J, Garcia I, Gomez-Vallejo V, Llop J and Penades S (2014). "(68)ga-labeled gold glyconanoparticles for exploring blood-brain barrier permeability: Preparation, biodistribution studies, and improved brain uptake via neuropeptide conjugation". *Journal of the American Chemical Society* 136(1): 449-457.

Gantner BN, Simmons RM, Canavera SJ, Akira S and Underhill DM (2003). "Collaborative induction of inflammatory responses by dectin-1 and toll-like receptor 2". *Journal of Experimental Medicine* 197(9): 1107-1117.

Geiser M, Rothen-Rutishauser B, Kapp N, Schurch S, Kreyling W, Schulz H, Semmler M, Im Hof V, Heyder J and Gehr P (2005). "Ultrafine particles cross cellular membranes by nonphagocytic mechanisms in lungs and in cultured cells". *Environmental Health Perspectives* 113(11): 1555-1560.

Geraci C, Heidel D, Sayes C, Hodson L, Schulte P, Eastlake A and Brenner S (2015). "Perspectives on the design of safer nanomaterials and manufacturing processes". *Journal of Nanoparticle Research* 17(9).

Geraets L, Oomen AG, Schroeter JD, Coleman VA and Cassee FR (2012). "Tissue distribution of inhaled micro- and nano-sized cerium oxide particles in rats: Results from a 28-day exposure study". *Toxicological Sciences* 127(2): 463-473.

Geraets L, Oomen AG, Krystek P, Jacobsen NR, Wallin H, Laurentie M, Verharen HW, Brandon EF and de Jong WH (2014). "Tissue distribution and elimination after oral and intravenous administration of different titanium dioxide nanoparticles in rats". *Particle and Fibre Toxicology* 11: 30.

Gilkey MJ, Krishnan V, Scheetz L, Jia X, Rajasekaran AK and Dhurjati PS (2015). "Physiologically based pharmacokinetic modeling of fluorescently labeled block copolymer nanoparticles for controlled drug delivery in leukemia therapy". *CPT: pharmacometrics & systems pharmacology* 4(3): e00013.

Gliga AR, Skoglund S, Wallinder IO, Fadeel B and Karlsson HL (2014). "Size-dependent cytotoxicity of silver nanoparticles in human lung cells: The role of cellular uptake, agglomeration and ag release". *Particle and Fibre Toxicology* 11.

Gordon S and Taylor PR (2005). "Monocyte and macrophage heterogeneity". *Nature Reviews Immunology* 5(12): 953-964.

Graham UM, Tseng MT, Jasinski JB, Yokel RA, Unrine JM, Davis BH, Dozier AK, Hardas SS, Sultana R, Grulke EA and Allan Butterfield D (2014). "In vivo processing of ceria nanoparticles inside liver: Impact on free-radical scavenging activity and oxidative stress". *ChemPlusChem* 79(8): 1083-1088.

Grosse Y, Loomis D, Guyton KZ, Lauby-Secretan B, El Ghissassi F, Bouvard V, Benbrahim-Tallaa L, Guha N, Scoccianti C, Mattock H, Straif K and Grp IARCM (2014). "Carcinogenicity of fluoro-edenite, silicon carbide fibres and whiskers, and carbon nanotubes". *Lancet Oncology* 15(13): 1427-1428.

Guha A (2008). "Transport and deposition of particles in turbulent and laminar flow". *Annual Review of Fluid Mechanics* 40: 311-341.

Guo SJ, Zhang S and Sun SH (2013). "Tuning nanoparticle catalysis for the oxygen reduction reaction". *Angewandte Chemie-International Edition* 52(33): 8526-8544.

Halliwell B and Gutteridge JMC (2015). "*Free radicals in biology and medicine."*, Oxford University Press.

Hardas SS, Butterfield DA, Sultana R, Tseng MT, Dan M, Florence RL, Unrine JM, Graham UM, Wu P, Grulke EA and Yokel RA (2010). "Brain distribution and toxicological evaluation of a systemically delivered engineered nanoscale ceria". *Toxicological sciences : an official journal of the Society of Toxicology* 116(2): 562-576.

Harmsen AG, Muggenburg BA, Snipes MB and Bice DE (1985). "The role of macrophages in particle translocation from lungs to lymph-nodes". *Science* 230(4731): 1277-1280.

He X, Zhang H, Ma Y, Bai W, Zhang Z, Lu K, Ding Y, Zhao Y and Chai Z (2010). "Lung deposition and extrapulmonary translocation of nano-ceria after intratracheal instillation". *Nanotechnology* 21(28): 285103.

Heckman KL, DeCoteau W, Estevez A, Reed KJ, Costanzo W, Sanford D, Leiter JC, Clauss J, Knapp K, Gomez C, Mullen P, Rathbun E, Prime K, Marini J, Patchefsky J, Patchefsky AS, Hailstone RK and Erlichman JS (2013). "Custom cerium oxide nanoparticles protect against a free radical mediated autoimmune degenerative disease in the brain". *ACS Nano* 7(12): 10582-10596.

Hinderliter PM, Minard KR, Orr G, Chrisler WB, Thrall BD, Pounds JG and Teeguarden JG (2010). "Isdd: A computational model of particle sedimentation, diffusion and target cell dosimetry for in vitro toxicity studies". *Particle and Fibre Toxicology* 7(1): 36.

Hirn S, Semmler-Behnke M, Schleh C, Wenk A, Lipka J, Schaffler M, Takenaka S, Moller W, Schmid G, Simon U and Kreyling WG (2011). "Particle size-dependent and surface charge-dependent biodistribution of gold nanoparticles after intravenous administration". *Eur J Pharm Biopharm* 77(3): 407-416.

Hofmann W (2011). "Modelling inhaled particle deposition in the human lung-a review". *Journal of Aerosol Science* 42(10): 693-724.

Hussain SM, Warheit DB, Ng SP, Comfort KK, Grabinski CM and Braydich-Stolle LK (2015). "At the crossroads of nanotoxicology in vitro: Past achievements and current challenges". *Toxicological Sciences* 147(1): 5-16.

Hyafil F, Cornily JC, Feig JE, Gordon R, Vucic E, Amirbekian V, Fisher EA, Fuster V, Feldman LJ and Fayad ZA (2007). "Noninvasive detection of macrophages using a nanoparticulate contrast agent for computed tomography". *Nature Materials* 13(5): 636-641.

Illum L, Thomas NW and Davis SS (1986). "Effect of a selected suppression of the reticuloendothelial system on the distribution of model carrier particles". *Journal of Pharmaceutical Sciences* 75(1): 16-22.

Illum L and Davis SS (1987). "Targeting of colloidal particles to the bone marrow". *Life Sciences* 40(16): 1553-1560.

IPCS (2010). "*Characterization and application of physiologically based pharmacokinetic models in risk assessment "*, World Health Organization, WHO.

ISO (2008) "ISO/TS 27687:2008, nanotechnologies —terminology and definitions for nano-objects — nanoparticle, nanofibre and nanoplate ". ISO International Organisation for Standardisation.

James K, Highsmith J and Evers P (2014) "Nanotechnology market - nanotechnology markets in healthcare & medicine ". *Drug Development & Devlivery*.

Jiang JK, Oberdorster G and Biswas P (2009). "Characterization of size, surface charge, and agglomeration state of nanoparticle dispersions for toxicological studies". *Journal of Nanoparticle Research* 11(1): 77-89.

Jiang W, Kim BY, Rutka JT and Chan WC (2008). "Nanoparticle-mediated cellular response is size-dependent". *Nature Nanotechnology* 3(3): 145-150.

Jin H, Heller DA, Sharma R and Strano MS (2009). "Size-dependent cellular uptake and expulsion of single-walled carbon nanotubes: Single particle tracking and a generic uptake model for nanoparticles". *ACS Nano* 3(1): 149-158.

Johanson G and Rauma M (2008). "Basis for skin notation. Part 1. Dermal penetration data for substances on the swedish oel list.". *Arbete och Hälsa* 42(2): 1-235.

Johanson G, Ed. (2014). "*Modeling of disposition in: Reference module in biomedical sciences"*, Elsevier.

Johanson G and Carlander U (2016) "Uptake and biodistribution of nanoparticles – a review.". KEMI Swedish Chemicals Agency. Rapport 12/16 - article number: 361 211.

Keene AM, Peters D, Rouse R, Stewart S, Rosen ET and Tyner KM (2012). "Tissue and cellular distribution of gold nanoparticles varies based on aggregation/agglomeration status". *Nanomedicine* 7(2): 199-209.

Keller J, Wohlleben W, Ma-Hock L, Strauss V, Groters S, Kuttler K, Wiench K, Herden C, Oberdorster G, van Ravenzwaay B and Landsiedel R (2014). "Time course of lung retention and toxicity of inhaled particles: Short-term exposure to nano-ceria". *Archives of toxicology* 88(11): 2033-2059.

Kermanizadeh A, Balharry D, Wallin H, Loft S and Moller P (2015). "Nanomaterial translocation-the biokinetics, tissue accumulation, toxicity and fate of materials in secondary organs-a review". *Critical reviews in toxicology*: 1-36.

Knop K, Hoogenboom R, Fischer D and Schubert US (2010). "Poly(ethylene glycol) in drug delivery: Pros and cons as well as potential alternatives". *Angewandte Chemie* 49(36): 6288-6308.

Kolanjiyil AV and Kleinstreuer C (2013). "Nanoparticle mass transfer from lung airways to systemic regions--part ii: Multi-compartmental modeling". *Journal of biomechanical engineering* 135(12): 121004.

Kolhar P, Anselmo AC, Gupta V, Pant K, Prabhakarpandian B, Ruoslahti E and Mitragotri S (2013). "Using shape effects to target antibody-coated nanoparticles to lung and brain endothelium". *Proceedings of the National Academy of Sciences of the United States of America* 110(26): 10753-10758.

Konduru NV, Jimenez RJ, Swami A, Friend S, Castranova V, Demokritou P, Brain JD and Molina RM (2015a). "Silica coating influences the corona and biokinetics of cerium oxide nanoparticles". *Particle and fibre toxicology* 12: 31.

Konduru NV, Jimenez RJ, Swami A, Friend S, Castranova V, Demokritou P, Brain JD and Molina RM (2015b). "Silica coating influences the corona and biokinetics of cerium oxide nanoparticles". *Particle and Fibre Toxicology* 12.

Konduru NV, Jimenez RJ, Swami A, Friend S, Castranova V, Demokritou P, Brain JD and Molina RM (2016). "Silica coating influences the corona and biokinetics of cerium oxide nanoparticles (vol 12, 31, 2015)". *Particle and Fibre Toxicology* 13.

Korani M, Rezayat SM, Gilani K, Arbabi Bidgoli S and Adeli S (2011). "Acute and subchronic dermal toxicity of nanosilver in guinea pig". *International Journal of Nanomedicine* 6: 855-862.

Kreyling WG, Semmler-Behnke M, Takenaka S and Moller W (2013). "Differences in the biokinetics of inhaled nano- versus micrometer-sized particles". *Accounts of chemical research* 46(3): 714-722.

Krishnan K and Andersen ME (2010). "*Quantitative modeling in toxicology"*. West Sussex, John Wiley & Sons Ltd.

Krug HF and Wick P (2011). "Nanotoxicology: An interdisciplinary challenge". *Angewandte Chemie International Edition in English* 50(6): 1260-1278.

Kumari M, Kumari SI and Grover P (2014a). "Genotoxicity analysis of cerium oxide micro and nanoparticles in wistar rats after 28 days of repeated oral administration". *Mutagenesis* 29(6): 467-479.

Kumari M, Kumari SI, Kamal SSK and Grover P (2014b). "Genotoxicity assessment of cerium oxide nanoparticles in female wistar rats after acute oral exposure". *Mutation Research-Genetic Toxicology and Environmental Mutagenesis* 775: 7-19.

Lacerda L, Herrero MA, Venner K, Bianco A, Prato M and Kostarelos K (2008). "Carbon-nanotube shape and individualization critical for renal excretion". *Small* 4(8): 1130-1132.

Lai SK, Wang YY and Hanes J (2009). "Mucus-penetrating nanoparticles for drug and gene delivery to mucosal tissues". *Advanced Drug Delivery Reviews* 61(2): 158-171.

Lang CH, Bagby GJ, Dobrescu C, Ottlakan A and Spitzer JJ (1992). "Sepsis- and endotoxin-induced increase in organ glucose uptake in leukocyte-depleted rats". *American Journal of Physiology* 263(6 Pt 2): R1324-1332.

Lankveld DP, Oomen AG, Krystek P, Neigh A, Troost-de Jong A, Noorlander CW, Van Eijkeren JC, Geertsma RE and De Jong WH (2010). "The kinetics of the tissue distribution of silver nanoparticles of different sizes". *Biomaterials* 31(32): 8350-8361.

Larsen A, Stoltenberg M and Danscher G (2007). "In vitro liberation of charged gold atoms: Autometallographic tracing of gold ions released by macrophages grown on metallic gold surfaces". *Histochemistry and cell biology* 128(1): 1-6.

Lee CH, Cheng SH, Wang YJ, Chen YC, Chen NT, Souris J, Chen CT, Mou CY, Yang CS and Lo LW (2009a). "Near-infrared mesoporous silica nanoparticles for optical imaging: Characterization and in vivo biodistribution". *Advanced Functional Materials* 19(2): 215-222.

Lee HA, Leavens TL, Mason SE, Monteiro-Riviere NA and Riviere JE (2009b). "Comparison of quantum dot biodistribution with a blood-flow-limited physiologically based pharmacokinetic model". *Nano Letters* 9(2): 794-799.

Lee J, Mahendra S and Alvarez PJJ (2010). "Nanomaterials in the construction industry: A review of their applications and environmental health and safety considerations". *ACS Nano* 4(7): 3580-3590.

Lesniak A, Fenaroli F, Monopoli MP, Aberg C, Dawson KA and Salvati A (2012). "Effects of the presence or absence of a protein corona on silica nanoparticle uptake and impact on cells". *ACS Nano* 6(7): 5845-5857.

Levick JR (2010). "*An introduction to cardiovascular physiology"*. London, Hodder Arnold.

Li D, Johanson G, Emond C, Carlander U, Philbert M and Jolliet O (2014). "Physiologically based pharmacokinetic modeling of polyethylene glycol-coated polyacrylamide nanoparticles in rats". *Nanotoxicology* 8(S1): 128–137.

Li D, Morishita M, Wagner JG, Fatouraie M, Wooldridge M, Eagle WE, Barres J, Carlander U, Emond C and Jolliet O (2016). "In vivo biodistribution and physiologically based pharmacokinetic modeling of inhaled fresh and aged cerium oxide nanoparticles in rats". *Particle and Fibre Toxicology* 13(1): 45.

Li M, Al-Jamal KT, Kostarelos K and Reineke J (2010). "Physiologically based pharmacokinetic modeling of nanoparticles". *ACS Nano* 4(11): 6303-6317.

Li M and Reineke J (2011). "Mathemathical modelling of nanoparticle biodistribution: Extrapolation among intravenous, oral and pulmonary administration routes". *International Journal of Nano and Biomaterials* 3(3): 222-238.

Li M, Panagi Z, Avgoustakis K and Reineke J (2012). "Physiologically based pharmacokinetic modeling of plga nanoparticles with varied mpeg content". *International Journal of Nanomedicine* 7: 1345-1356.

Limbach LK, Wick P, Manser P, Grass RN, Bruinink A and Stark WJ (2007). "Exposure of engineered nanoparticles to human lung epithelial cells: Influence of chemical composition and catalytic activity on oxidative stress". *Environmental Science & Technology* 41(11): 4158-4163.

Lin IC, Liang M, Liu TY, Monteiro MJ and Toth I (2012). "Cellular transport pathways of polymer coated gold nanoparticles". *Nanomedicine* 8(1): 8-11.

Lin P, Chen JW, Chang LW, Wu JP, Redding L, Chang H, Yeh TK, Yang CS, Tsai MH, Wang HJ, Kuo YC and Yang RS (2008). "Computational and ultrastructural toxicology of a nanoparticle, quantum dot 705, in mice". *Environmental science & technology* 42(16): 6264-6270.

Lin Z, Monteiro-Riviere NA and Riviere JE (2015a). "A physiologically based pharmacokinetic model for polyethylene glycol-coated gold nanoparticles of different sizes in adult mice". *Nanotoxicology*: 1-11.

Lin Z, Monteiro-Riviere NA, Kannan R and Riviere JE (2016). "A computational framework for interspecies pharmacokinetics, exposure and toxicity assessment of gold nanoparticles". *Nanomedicine* 11(2): 107-119.

Lin ZM, Monteiro-Riviere NA and Riviere JE (2015b). "Pharmacokinetics of metallic nanoparticles". *Wiley Interdisciplinary Reviews-Nanomedicine and Nanobiotechnology* 7(2): 189-217.

Liou SH, Tsai CS, Pelclova D, Schubauer-Berigan MK and Schulte PA (2015). "Assessing the first wave of epidemiological studies of nanomaterial workers". *Journal of nanoparticle research : an interdisciplinary forum for nanoscale science and technology* 17: 413.

Liu JW, Chen LF, Cui H, Zhang JY, Zhang L and Su CY (2014). "Applications of metal-organic frameworks in heterogeneous supramolecular catalysis". *Chemical Society Reviews* 43(16): 6011-6061.

Loeschner K, Hadrup N, Qvortrup K, Larsen A, Gao X, Vogel U, Mortensen A, Lam HR and Larsen EH (2011). "Distribution of silver in rats following 28 days of repeated oral exposure to silver nanoparticles or silver acetate". *Particle and Fibre Toxicology* 8: 18.

Luciani N, Gazeau F and Wilhelm C (2009). "Reactivity of the monocyte/macrophage system to superparamagnetic anionic nanoparticles". *Journal of Materials Chemistry* 19(35): 6373-6380.

Lundqvist M, Stigler J, Elia G, Lynch I, Cedervall T and Dawson KA (2008). "Nanoparticle size and surface properties determine the protein corona with possible implications for biological impacts". *PNAS Proceedings of the National Academy of Sciences of the United States of America* 105(38): 14265-14270.

MacCalman L, Tran CL and Kuempel E (2009). "Development of a bio-mathematical model in rats to describe clearance, retention and translocation of inhaled nano particles throughout the body". *Journal of Physics:Conference Series* 151.

Magdolenova Z, Collins A, Kumar A, Dhawan A, Stone V and Dusinska M (2014). "Mechanisms of genotoxicity. A review of in vitro and in vivo studies with engineered nanoparticles". *Nanotoxicology* 8(3): 233-278.

Mager DE, Mody V, Xu C, Forrest A, Lesniak WG, Nigavekar SS, Kariapper MT, Minc L, Khan MK and Balogh LP (2012). "Physiologically based pharmacokinetic model for composite nanodevices: Effect of charge and size on in vivo disposition". *Pharmaceutical Research* 29(9): 2534-2542.

Mahler GJ, Esch MB, Tako E, Southard TL, Archer SD, Glahn RP and Shuler ML (2012). "Oral exposure to polystyrene nanoparticles affects iron absorption". *Nature Nanotechnology* 7(4): 264-U1500.

Mahon E, Hristov DR and Dawson KA (2012). "Stabilising fluorescent silica nanoparticles against dissolution effects for biological studies". *Chem Commun (Camb)* 48(64): 7970-7972.

Manke A, Wang L and Rojanasakul Y (2013). "Mechanisms of nanoparticle-induced oxidative stress and toxicity". *BioMed research international* 2013: 942916.

Marquis BJ, Love SA, Braun KL and Haynes CL (2009). "Analytical methods to assess nanoparticle toxicity". *Analyst* 134(3): 425-439.

McCracken C, Dutta PK and Waldman WJ (2016). "Critical assessment of toxicological effects of ingested nanoparticles". *Environmental Science-Nano* 3(2): 256-282.

Mehta D and Malik AB (2006). "Signaling mechanisms regulating endothelial permeability". *Physiological Reviews* 86(1): 279-367.

Mei L, Zhang Z, Zhao L, Huang L, Yang XL, Tang J and Feng SS (2013). "Pharmaceutical nanotechnology for oral delivery of anticancer drugs". *Advanced Drug Delivery Reviews* 65(6): 880-890.

Michalet X, Pinaud FF, Bentolila LA, Tsay JM, Doose S, Li JJ, Sundaresan G, Wu AM, Gambhir SS and Weiss S (2005). "Quantum dots for live cells, in vivo imaging, and diagnostics". *Science* 307(5709): 538-544.

Michel CC and Curry FE (1999). "Microvascular permeability". *Physiological Reviews* 79(3): 703-761.

Midander K, Julander A, Kettelarij J and Liden C (2016). "Testing in artificial sweat - is less more? Comparison of metal release in two different artificial sweat solutions". *Regulatory Toxicology and Pharmacology* 81: 381-386.

Mishra N, Tiwari S, Vaidya B, Agrawal GP and Vyas SP (2011). "Lectin anchored plga nanoparticles for oral mucosal immunization against hepatitis b". *Journal of Drug Targeting* 19(1): 67-78.

Misra SK, Dybowska A, Berhanu D, Luoma SN and Valsami-Jones E (2012). "The complexity of nanoparticle dissolution and its importance in nanotoxicological studies". *The Science of the total environment* 438: 225-232.

Moghimi SM (2002). "Chemical camouflage of nanospheres with a poorly reactive surface: Towards development of stealth and target-specific nanocarriers". *Biochimica et biophysica acta* 1590(1-3): 131-139.

Mohr F, Ed. (2009). "*Gold chemistry - applications and future directions in the life sciences"*, WILEY-VCH Verlag GmbH & Co. KGaA.

Molina RM, Konduru NV, Jimenez RJ, Pyrgiotakis G, Demokritou P, Wohlleben W and Brain JD (2014). "Bioavailability, distribution and clearance of tracheally instilled, gavaged or injected cerium dioxide nanoparticles and ionic cerium". *Environmental Science-Nano* 1(6): 561-573.

Monopoli MP, Aberg C, Salvati A and Dawson KA (2012). "Biomolecular coronas provide the biological identity of nanosized materials". *Nature Nanotechnology* 7(12): 779-786.

Morais T, Soares ME, Duarte JA, Soares L, Maia S, Gomes P, Pereira E, Fraga S, Carmo H and Bastos Mde L (2012). "Effect of surface coating on the biodistribution profile of gold nanoparticles in the rat". *European Journal of Pharmaceutics and Biopharmaceutics* 80(1): 185-193.

Morfeld P, Bruch J, Levy L, Ngiewih Y, Chaudhuri I, Muranko HJ, Myerson R and McCunney RJ (2016). "Response to the reply on behalf of the 'permanent senate commission for the investigation of health hazards of chemical compounds in the work area' (mak commission) by andrea hartwig karlsruhe institute of technology (kit)". *Particle and Fibre Toxicology* 13.

Morrow PE (1988). "Possible mechanisms to explain dust overloading of the lungs". *Fundamental and Applied Toxicology* 10(3): 369-384.

Morrow PE, Haseman JK, Hobbs CH, Driscoll KE, Vu V and Oberdorster G (1996). "The maximum tolerated dose for inhalation bioassays: Toxicity vs overload". *Fundamental and Applied Toxicology* 29(2): 155-167.

Moyes SM, Smyth SH, Shipman A, Long S, Morris JF and Carr KE (2007). "Parameters influencing intestinal epithelial permeability and microparticle uptake in vitro". *International Journal of Pharmaceutics* 337(1-2): 133-141.

Muhlfeld C, Rothen-Rutishauser B, Blank F, Vanhecke D, Ochs M and Gehr P (2008). "Interactions of nanoparticles with pulmonary structures and cellular responses". *American Journal of Physiology-Lung Cellular and Molecular Physiology* 294(5): L817-L829.

Nalabotu SK, Kolli MB, Triest WE, Ma JY, Manne ND, Katta A, Addagarla HS, Rice KM and Blough ER (2011). "Intratracheal instillation of cerium oxide nanoparticles induces hepatic toxicity in male sprague-dawley rats". *International Journal of Nanomedicine* 6: 2327-2335.

Nel A, Xia T, Madler L and Li N (2006). "Toxic potential of materials at the nanolevel". *Science* 311(5761): 622-627.

Nel AE, Madler L, Velegol D, Xia T, Hoek EM, Somasundaran P, Klaessig F, Castranova V and Thompson M (2009). "Understanding biophysicochemical interactions at the nano-bio interface". *Nature Materials* 8(7): 543-557.

Nowack B, Brouwer C, Geertsma RE, Heugens EHW, Ross BL, Toufektsian MC, Wijnhoven SWP and Aitken RJ (2013). "Analysis of the occupational, consumer and environmental exposure to engineered nanomaterials used in 10 technology sectors". *Nanotoxicology* 7(6): 1152-1156.

Oberdorster G, Maynard A, Donaldson K, Castranova V, Fitzpatrick J, Ausman K, Carter J, Karn B, Kreyling W, Lai D, Olin S, Monteiro-Riviere N, Warheit D and Yang H (2005a). "Principles for characterizing the potential human health effects from exposure to nanomaterials: Elements of a screening strategy". *Particle and Fibre Toxicology* 2: 8.

Oberdorster G, Oberdorster E and Oberdorster J (2005b). "Nanotoxicology: An emerging discipline evolving from studies of ultrafine particles". *Environ Health Perspect* 113(7): 823-839.

Oberdörster G (1988). "Lung clearance of inhaled insoluble and soluble particles.". *Journal of Aerosol Medicine* 1(4): 289-330.

OECD (2012) "Guidance on sample preparation and dosimetry for the safety testing of manufactured nanomaterials". ENV/JM/MONO(2012)40.

OECD. (2016). "Safety of manufactured nanomaterials." from http://www.oecd.org/science/nanosafety/.

Ogawara K, Furumoto K, Takakura Y, Hashida M, Higaki K and Kimura T (2001). "Surface hydrophobicity of particles is not necessarily the most important determinant in their in vivo disposition after intravenous administration in rats". *Journal of Controlled Release* 77(3): 191-198.

Ohta S, Inasawa S and Yamaguchi Y (2012). "Real time observation and kinetic modeling of the cellular uptake and removal of silicon quantum dots". *Biomaterials* 33(18): 4639-4645.

Opitz AW, Wickstrom E, Thakur ML and Wagner NJ (2010). "Physiologically based pharmacokinetics of molecular imaging nanoparticles for mrna detection determined in tumor-bearing mice". *Oligonucleotides* 20(3): 117-125.

Park EJ, Park YK and Park K (2009). "Acute toxicity and tissue distribution of cerium oxide nanoparticles by a single oral administration in rats ". *Toxicological Research KSOT* 25(2): 79-84

Park EJ, Yi J, Kim Y, Choi K and Park K (2010). "Silver nanoparticles induce cytotoxicity by a trojan-horse type mechanism". *Toxicology in Vitro* 24(3): 872-878.

Parveen S, Misra R and Sahoo SK (2012). "Nanoparticles: A boon to drug delivery, therapeutics, diagnostics and imaging". *Nanomedicine : nanotechnology, biology, and medicine* 8(2): 147-166.

Paulsson M, Krag C, Frederiksen T and Brandbyge M (2009). "Conductance of alkanedithiol single-molecule junctions: A molecular dynamics study". *Nano Letters* 9(1): 117-121.

Pauluhn J (2014). "Derivation of occupational exposure levels (oels) of low-toxicity isometric biopersistent particles: How can the kinetic lung overload paradigm be used for improved inhalation toxicity study design and oel-derivation?". *Particle and Fibre Toxicology* 11(1): 72.

Peng B, Andrews J, Nestorov I, Brennan B, Nicklin P and Rowland M (2001). "Tissue distribution and physiologically based pharmacokinetics of antisense phosphorothioate oligonucleotide isis 1082 in rat". *Antisense & nucleic acid drug development* 11(1): 15-27.

Pery AR, Brochot C, Hoet PH, Nemmar A and Bois FY (2009). "Development of a physiologically based kinetic model for 99m-technetium-labelled carbon nanoparticles inhaled by humans". *Inhalation Toxicology* 21(13): 1099-1107.

Poland CA, Read SAK, Varet J, Carse G, Christensen FM and Hankin SM (2013). "*Dermal absorption of nanomaterials. "*. Copenhagen.

Qu X, Alvarez PJ and Li Q (2013). "Applications of nanotechnology in water and wastewater treatment". *Water Research* 47(12): 3931-3946.

Raj S, Jose S, Sumod US and Sabitha M (2012). "Nanotechnology in cosmetics: Opportunities and challenges". *Journal of pharmacy & bioallied sciences* 4(3): 186-193.

Reddy LH, Arias JL, Nicolas J and Couvreur P (2012). "Magnetic nanoparticles: Design and characterization, toxicity and biocompatibility, pharmaceutical and biomedical applications". *Chemical reviews* 112(11): 5818-5878.

Rehberg M, Nekolla K, Sellner S, Praetner M, Mildner K, Zeuschner D and Krombach F (2016). "Intercellular transport of nanomaterials is mediated by membrane nanotubes in vivo". *Small* 12(14): 1882-1890.

RIVM NIfPHatE (2002) " Multiple path particle dosimetry model (mppd v 1.0): A model for human and rat airway particle dosimetry. ". Bilthoven, The Netherlands. RIVA Report 650010030.

Roduner E (2006). "Size matters: Why nanomaterials are different". *Chemical Society Reviews* 35(7): 583-592.

Roger E, Lagarce F, Garcion E and Benoit JP (2010). "Biopharmaceutical parameters to consider in order to alter the fate of nanocarriers after oral delivery". *Nanomedicine (Lond)* 5(2): 287-306.

Saba TM and Di Luzio NR (1969). "Reticuloendothelial blockade and recovery as a function of opsonic activity". *American Journal of Physiology* 216(1): 197-205.

Saba TM (1970). "Physiology and physiopathology of the reticuloendothelial system". *Archives of Internal Medicine* 126(6): 1031-1052.

Sabella S, Carney RP, Brunetti V, Malvindi MA, Al-Juffali N, Vecchio G, Janes SM, Bakr OM, Cingolani R, Stellacci F and Pompa PP (2014). "A general mechanism for intracellular toxicity of metal-containing nanoparticles". *Nanoscale* 6(12): 7052-7061.

Sadauskas E, Danscher G, Stoltenberg M, Vogel U, Larsen A and Wallin H (2009). "Protracted elimination of gold nanoparticles from mouse liver". *Nanomedicine : nanotechnology, biology, and medicine* 5(2): 162-169.

Sahay G, Alakhova DY and Kabanov AV (2010). "Endocytosis of nanomedicines". *Journal of Controlled Release* 145(3): 182-195.

Sarin H (2010). "Physiologic upper limits of pore size of different blood capillary types and another perspective on the dual pore theory of microvascular permeability". *Journal of Angiogenesis Research* 2: 14.

Schmid O and Stoeger T (2016). "Surface area is the biologically most effective dose metric for acute nanoparticle toxicity in the lung". *Journal of Aerosol Science* 99: 133-143.

Scholl JA, Koh AL and Dionne JA (2012). "Quantum plasmon resonances of individual metallic nanoparticles". *Nature* 483(7390): 421-U468.

Schottler S, Becker G, Winzen S, Steinbach T, Mohr K, Landfester K, Mailander V and Wurm FR (2016). "Protein adsorption is required for stealth effect of poly(ethylene glycol)- and poly(phosphoester)-coated nanocarriers". *Nature Nanotechnology* 11(4): 372-377.

Schulze C, Schaefer UF, Ruge CA, Wohlleben W and Lehr CM (2011). "Interaction of metal oxide nanoparticles with lung surfactant protein a". *European journal of pharmaceutics and biopharmaceutics : official journal of Arbeitsgemeinschaft fur Pharmazeutische Verfahrenstechnik e.V* 77(3): 376-383.

Semmler-Behnke M, Takenaka S, Fertsch S, Wenk A, Seitz J, Mayer P, Oberdorster G and Kreyling WG (2007). "Efficient elimination of inhaled nanoparticles from the alveolar region: Evidence for interstitial uptake and subsequent reentrainment onto airway epithelium". *Environmental Health Perspectives* 115(5): 728-733.

Setyawati MI, Tay CY, Docter D, Stauber RH and Leong DT (2015). "Understanding and exploiting nanoparticles' intimacy with the blood vessel and blood". *Chemical Society Reviews* 44(22): 8174-8199.

Sharifi S, Behzadi S, Laurent S, Forrest ML, Stroeve P and Mahmoudi M (2012). "Toxicity of nanomaterials". *Chemical Society Reviews* 41(6): 2323-2343.

Snipes MB, Boecker BB and McClellan RO (1983). "Retention of monodisperse or polydisperse aluminosilicate particles inhaled by dogs, rats, and mice". *Toxicology and Applied Pharmacology* 69(3): 345-362.

Snipes MB (1989). "Long-term retention and clearance of particles inhaled by mammalian species". *Critical reviews in toxicology* 20(3): 175-211.

Sonavane G, Tomoda K and Makino K (2008). "Biodistribution of colloidal gold nanoparticles after intravenous administration: Effect of particle size". *Colloids and Surfaces B: Biointerfaces* 66(2): 274-280.

Stern ST, Adiseshaiah PP and Crist RM (2012). "Autophagy and lysosomal dysfunction as emerging mechanisms of nanomaterial toxicity". *Particle and Fibre Toxicology* 9.

Sweeney LM, MacCalman L, Haber LT, Kuempel ED and Tran CL (2015). "Bayesian evaluation of a physiologically-based pharmacokinetic (pbpk) model of long-term kinetics of metal nanoparticles in rats". *Regulatory Toxicology and Pharmacology* 73(1): 151-163.

Teeguarden JG, Hinderliter PM, Orr G, Thrall BD and Pounds JG (2007). "Particokinetics in vitro: Dosimetry considerations for in vitro nanoparticle toxicity assessments". *Toxicological sciences : an official journal of the Society of Toxicology* 95(2): 300-312.

Tenzer S, Docter D, Kuharev J, Musyanovych A, Fetz V, Hecht R, Schlenk F, Fischer D, Kiouptsi K, Reinhardt C, Landfester K, Schild H, Maskos M, Knauer SK and Stauber RH (2013). "Rapid formation of plasma protein corona critically affects nanoparticle pathophysiology". *Nature Nanotechnology* 8(10): 772-781.

Tinkle SS, Antonini JM, Rich BA, Roberts JR, Salmen R, DePree K and Adkins EJ (2003). "Skin as a route of exposure and sensitization in chronic beryllium disease". *Environmental Health Perspectives* 111(9): 1202-1208.

Tran CL, Buchanan D, Cullen RT, Searl A, Jones AD and Donaldson K (2000). "Inhalation of poorly soluble particles. Ii. Influence of particle surface area on inflammation and clearance". *Inhalation Toxicology* 12(12): 1113-1126.

Travlos GS (2006). "Normal structure, function, and histology of the bone marrow". *Toxicologic pathology* 34(5): 548-565.

Utembe W, Potgieter K, Stefaniak AB and Gulumian M (2015). "Dissolution and biodurability: Important parameters needed for risk assessment of nanomaterials". *Particle and Fibre Toxicology* 12: 11.

Vallhov H, Qin J, Johansson SM, Ahlborg N, Muhammed MA, Scheynius A and Gabrielsson S (2006). "The importance of an endotoxin-free environment during the production of nanoparticles used in medical applications". *Nano Letters* 6(8): 1682-1686.

van der Zande M, Vandebriel RJ, Van Doren E, Kramer E, Herrera Rivera Z, Serrano-Rojero CS, Gremmer ER, Mast J, Peters RJ, Hollman PC, Hendriksen PJ, Marvin HJ, Peijnenburg AA and Bouwmeester H (2012). "Distribution, elimination, and toxicity of silver nanoparticles and silver ions in rats after 28-day oral exposure". *ACS Nano* 6(8): 7427-7442.

van Furth R (1989). "Origin and turnover of monocytes and macrophages". *Current topics in pathology. Ergebnisse der Pathologie* 79: 125-150.

van Schooneveld MM, Vucic E, Koole R, Zhou Y, Stocks J, Cormode DP, Tang CY, Gordon RE, Nicolay K, Meijerink A, Fayad ZA and Mulder WJ (2008). "Improved biocompatibility and pharmacokinetics of silica nanoparticles by means of a lipid coating: A multimodality investigation". *Nano Letters* 8(8): 2517-2525.

Wang L, Li YF, Zhou L, Liu Y, Meng L, Zhang K, Wu X, Zhang L, Li B and Chen C (2010). "Characterization of gold nanorods in vivo by integrated analytical techniques: Their uptake, retention, and chemical forms". *Analytical and Bioanalytical Chemistry* 396(3): 1105-1114.

Wang YL, Yuan LL, Yao CJ, Ding L, Li CC, Fang J, Sui KK, Liu YF and Wu MH (2014). "A combined toxicity study of zinc oxide nanoparticles and vitamin c in food additives". *Nanoscale* 6(24): 15333-15342.

Wang ZL and Wu W (2012). "Nanotechnology-enabled energy harvesting for self-powered micro-/nanosystems". *Angewandte Chemie* 51(47): 11700-11721.

Waser R (2012). "*Nanoelectronics and information technology "*. Weinheim, Germany, Wiley-VCH.

Wenger Y, Schneider RJ, 2nd, Reddy GR, Kopelman R, Jolliet O and Philbert MA (2011). "Tissue distribution and pharmacokinetics of stable polyacrylamide nanoparticles following intravenous injection in the rat". *Toxicology and Applied Pharmacology* 251(3): 181-190.

Verschoor CP, Puchta A and Bowdish DM (2012). "The macrophage". *Methods in molecular biology* 844: 139-156.

Wilhelm C, Gazeau F, Roger J, Pons JN and Bacri JC (2002). "Interaction of anionic superparamagnetic nanoparticles with cells: Kinetic analyses of membrane adsorption and subsequent internalization". *Langmuir* 18(21): 8148-8155.

Xia T, Kovochich M, Brant J, Hotze M, Sempf J, Oberley T, Sioutas C, Yeh JI, Wiesner MR and Nel AE (2006). "Comparison of the abilities of ambient and manufactured nanoparticles to induce cellular toxicity according to an oxidative stress paradigm". *Nano Lett* 6(8): 1794-1807.

Xu PA, Zeng GM, Huang DL, Feng CL, Hu S, Zhao MH, Lai C, Wei Z, Huang C, Xie GX and Liu ZF (2012). "Use of iron oxide nanomaterials in wastewater treatment: A review". *Science of the Total Environment* 424: 1-10.

Yokel R, Grulke E and MacPhail R (2013a). "Metal-based nanoparticle interactions with the nervous system: The challenge of brain entry and the risk of retention in the organism". *Wiley interdisciplinary reviews. Nanomedicine and nanobiotechnology* 5(4): 346-373.

Yokel RA, Florence RL, Unrine JM, Tseng MT, Graham UM, Wu P, Grulke EA, Sultana R, Hardas SS and Butterfield DA (2009). "Biodistribution and oxidative stress effects of a systemically-introduced commercial ceria engineered nanomaterial". *Nanotoxicology* 3(3): 234-248.

Yokel RA, Au TC, MacPhail R, Hardas SS, Butterfield DA, Sultana R, Goodman M, Tseng MT, Dan M, Haghnazar H, Unrine JM, Graham UM, Wu P and Grulke EA (2012). "Distribution, elimination, and biopersistence to 90 days of a systemically introduced 30 nm ceria-engineered nanomaterial in rats". *Toxicological sciences : an official journal of the Society of Toxicology* 127(1): 256-268.

Yokel RA, Tseng MT, Dan M, Unrine JM, Graham UM, Wu P and Grulke EA (2013b). "Biodistribution and biopersistence of ceria engineered nanomaterials: Size dependence". *Nanomedicine : nanotechnology, biology, and medicine* 9(3): 398-407.

Yokel RA, Unrine JM, Wu P, Wang BH and Grulke EA (2014). "Nanoceria biodistribution and retention in the rat after its intravenous administration are not greatly influenced by dosing schedule, dose, or particle shape". *Environmental Science-Nano* 1(6): 549-560.

Zhang X, Li W and Yang Z (2015). "Toxicology of nanosized titanium dioxide: An update". *Archives of toxicology* 89(12): 2207-2217.

Zhou XC, Xu WL, Liu GK, Panda D and Chen P (2010). "Size-dependent catalytic activity and dynamics of gold nanoparticles at the single-molecule level". *Journal of the American Chemical Society* 132(1): 138-146.

Zhu ZJ, Carboni R, Quercio MJ, Jr., Yan B, Miranda OR, Anderton DL, Arcaro KF, Rotello VM and Vachet RW (2010). "Surface properties dictate uptake, distribution, excretion, and toxicity of nanoparticles in fish". *Small* 6(20): 2261-2265.